### Precision Adaptive Hormone Control for Personalized Metastatic Prostate Cancer Treatment

Trung V. Phan,<sup>1</sup> Shengkai Li,<sup>2</sup> Benjamin Howe,<sup>2</sup> Sarah R. Amend,<sup>3</sup> Kenneth J. Pienta,<sup>3</sup> Joel S. Brown,<sup>4</sup> Robert A. Gatenby,<sup>4</sup> Constantine Frangakis,<sup>5,6</sup> Robert H. Austin,<sup>2</sup> and Ioannis G. Keverkidis<sup>1</sup>

<sup>1</sup>Department of Chemical and Biomolecular Engineering, John Hopkins University, Baltimore, MD 21218, USA

<sup>2</sup>Department of Physics,

Princeton University, Princeton, NJ 08544, USA

<sup>3</sup>Cancer Ecology Center, The Brady Urological Institute, Johns Hopkins School of Medicine, Baltimore, MD 21287, USA

<sup>4</sup>Departments of Radiology and Integrated Mathematical Oncology,

Moffitt Cancer Center, Tampa, FL 33612, USA

<sup>5</sup>Department of Medicine, Johns Hopkins University,

Baltimore, MD 21218, USA

<sup>6</sup>Department of Biostatistics, Bloomberg School of Public Health, Johns Hopkins University, Baltimore, MD 21218, USA

(Dated: October 22, 2024)

With the oncologist acting as the "game leader", we employ a Stackelberg game-theoretic model involving multiple populations to study prostate cancer. We refine the drug dosing schedule using an empirical Bayes feed-forward analysis, based on clinical data that reflects each patient's prostate-specific drug response. Our method-ology aims for a quantitative grasp of the parameter landscape of this adaptive multipopulation model, focusing on arresting the growth of drug-resistant prostate cancer by promoting competition across drug-sensitive cancer cell populations. Our findings indicate that not only is it is feasible to considerably extend cancer suppression duration through careful optimization, but even transform metastatic prostate cancer into a chronic condition instead of an acute one for most patients, with supporting clinical and analytical evidence.

#### I. INTRODUCTION

Although this study focuses on prostate cancer, the underlying principles can also be applied to various other cancers, especially those that are hormone-sensitive, such as breast or ovarian cancer. The focus is on the competition among populations within limited ecological niches and how these populations can be controlled. These ecologies are defined by their carrying capacities, which refer to the maximum number of organisms that the local environment's resources can sustain.

In the prostate gland, cells are responsive to male androgens, which function as resources regulating tissue cell death and proliferation. Under normal conditions, prostate tissue cells grow and die at rates dictated by androgen levels, maintaining glandular homeostasis. However, prostate cancer cells ignore these androgen limits, persist in their growth toward the gland's carrying capacity, and result in a larger tumor. When this local growth boundary is achieved, cancer cells may metastasize to different areas, where they form new environments with distinct carrying capacities. The coarse-grained characterization of these processes we employ in modeling metastatic cancer suggests that the body has a certain carrying capacity, which affects the general dynamics of tumor development and dissemination.

Hormone deprivation therapy aims to restrict proliferation and eliminate androgendependent prostate cells by removing androgen growth hormones. However, prostate cancer cells can develop resistance to this therapy, allowing them to continue dividing even without growth hormones. Resistant cells might (1) already exist within the prostate tumor before the initial treatment due to genetic or epigenetic diversity [1–3], or (2) arise as *de novo* resistant cells through a process of natural selection [4–7].

The two distinct cell types, which are either sensitive or resistant to androgens, can compete within a shared environment, creating a scenario akin to a resource game. Although the overall carrying capacity is dictated by the maximum number of cells that can occupy a particular environment, the proportion of androgen-sensitive and -resistant cells may vary based on their competitive interactions.

Testosterone serves as the primary male androgen. Androgens like testosterone attach to androgen receptors found on the surfaces of prostate cells. Through a complex signaling pathway, the occupation of these receptors stimulates the proliferation and apoptosis of androgen-sensitive cells. These cells, whose growth and demise are regulated by testosterone,

are referred to as T<sup>+</sup> cells due to their reliance on bound androgen receptors for growth and survival.

Over time, prostate tissue may develop, or may already contain, cells  $(T^{+/-})$  with an increased number of androgen receptors, which enhances their sensitivity to testosterone and allows them to proliferate with lower testosterone levels. Because these cells can thrive even when testosterone is reduced, they are labeled as "resistant" to leuprorelin, though their resistance is indirectly related to the drug. This resistance can progress, leading to the emergence or preexistence of prostate cancer cells that can grow entirely without testosterone, known as  $T^-$  cells. These cells are not effectively managed by standard androgen deprivation therapy, meaning that even when leuprorelin levels are elevated,  $T^-$  prostate cancer cells continue to proliferate.

As previously discussed, prostate cancer exhibits significant heterogeneity; our analysis focuses solely on differentiated cells and the PSA levels they produce. There is, however, a category of undifferentiated prostate cancer cells (PSA<sup> $-\loo$ </sup>) that do not secrete PSA, express stem cell markers, are resistant to androgen deprivation therapy, and demonstrate both high clonogenic capability and long-term tumor-propagating potential [8]. This is because they can progress to a differentiated state and divide asymmetrically to generate  $T^+$  cells. This process of de-differentiation and genuine evolution is beyond the scope of this paper.

The regulation of metastatic prostate cancer through adaptive hormone therapy employs the concentration of prostate-specific antigen (PSA) in the patient's body as an indicator of the number of cancer cells present. PSA, however, constitutes a flawed measure for quantifying prostate cells—encompassing both normal and malignant varieties [9, 10]. PSA is generated by both normal prostate cells and cancerous ones. An uptick in PSA levels in the bloodstream, which hints at unusual proliferation of prostate cells, prompts the initial therapeutic approach of administering leuprorelin. Leuprorelin functions as an agonist at the pituitary gland's gonadotropin-releasing hormone (GnRH) receptors, ultimately leading to a reduction in testosterone production by testicular cells, thereby inhibiting growth and leading to the apoptosis of T<sup>+</sup> prostate cells.

Patients with high levels of leuprorelin continued therapy are said to be "chemically castrated", but this is an entirely reversible condition if leuprorelin administration is ceased, unlike surgical castration.

One explanation for why patients undergoing chemical castration with leuprorelin ex-

hibit persistent PSA elevations in cases of metastatic castration-resistant prostate cancer (mCRPC) is that testosterone is also synthesized in the adrenal glands. To address this, abiraterone acetate is administered, which inhibits androgen synthesis in the adrenal glands, further diminishing testosterone levels beyond what is achieved with leuprorelin therapy alone. Abiraterone acts by inhibiting the CYP17A1 enzyme, essential for the production of androgens (male hormones) in the testes, adrenal glands, and prostate cancer tissue [11]. By blocking this enzyme, the drug significantly reduces the production of androgen steroid hormones, particularly testosterone, which plays a critical role in determining the proliferation capacity of these sensitive cells.

The patients we are concerned with here are all mCRPC patients who still have populations of  $T^+$ ,  $T^{+/-}$  and  $T^-$  cells. The task in this paper is to optimize the suppression of  $T^-$  cell growth through competition with  $T^+$  and  $T^{+/-}$  cells for mCRPC patients.

The concept of cancer adaptive chemotherapy [12] can be understood through the lens of Stackelberg sequential game theory [13]. Here, the oncologist leverages the ecological competition for shared resources among cancer cells, aiming to increase populations of drugsensitive subclones that, in turn, help inhibit the proliferation of drug-resistant ones [14, 15]. Instead of being seen as conclusive, the mathematical models employed to describe cancer population dynamics during treatment should be considered as heuristic tools. These provide oncologists with a framework to analytically grasp and influence cancer progression.

The effectiveness of adaptive chemotherapy arises from the competition among different cell populations for (1) a limited cell carrying capacity and (2) the extent to which cells compete with one another even when not close to the carrying capacity. In both scenarios (approaching the carrying capacity or inter-population competition), a more game-oriented dominant sub-population can hinder the growth of the game-oriented minority sub-population. Such game-oriented suppression can even prevent a quicker-reproducing, drug-resistant phenotype from expanding. In situations involving purely competitive suppression of growth rates near the carrying capacity, adaptive chemotherapy can delay the breakthrough of resistant cell populations, but it eventually falls short [16]. Nevertheless, as we will demonstrate, if the competition coefficients sufficiently favor the sensitive cells, it is feasible to indefinitely suppress resistant cell populations even when far from their carrying capacity.

In adaptive chemotherapy, the clinician dictates the treatment strategy through dose

scheduling. Ideally, both dose intensity and duration could be adjusted. However, if dose intensity remains fixed, then the PSA on-level and off-level serve as two modifiable trigger parameters to modify drug dosage. Currently, in clinical adaptive treatments, these adjustable parameters have not been optimized for maximum drug efficiency or response duration [12] and are instead set at an arbitrary 50% of the baseline PSA level [17].

As Hansen and Read have noted [16], it is feasible to select the PSA on-level for administering drugs to be above the initial baseline measurement at the start of treatment. This choice should ensure that the count of drug-sensitive cancer cells,  $T^+$ , approaches the total carrying capacity, while  $T^-$  remains significantly below it. In a straightforward model with two populations—where the first group, comprising  $T^+$  and  $T^{+/-}$ , is sensitive to drugs, and the second group, consisting only of  $T^-$ , is resistant—the PSA off-level should be nearly equal to the on-level. Both levels need to be near the carrying capacity to keep drug-sensitive cells close to their maximum and to limit the proliferation of drug-resistant cells.

These two concepts, (1) positioning the PSA trigger on level to maintain the total cell number near the total body carrying capacity and (2) setting the differential between on and off as small as possible are not new [16]. What we have further explored and propose here are:

- A systematic statistical approach to determine, from clinical data, important parameters describing cancer progression, including personalized growth rates and competition coefficients, as well as personalized parameters such as the initial number of cancer cells relative to carrying capacity and drug effectiveness, in the fundamental game theory model described in Section II. The details are provided in Section IV.
- The possibility, in favorable patient cases, of extending the period of cancer suppression below a threshold or even making prostate cancer chronic rather than progressive, albeit with continued therapy throughout the patient's lifetime. We show how these outcomes can be achieved via a *high level tight control* adaptive chemotherapy in Section V using Bayesian optimization. We provide analytical justifications and estimates for these findings, see Appendix B.

#### II. A SIMPLIFIED STACKELBERG GAME THEORY MODEL OF

#### ADAPTIVE THERAPY FOR PROSTATE CANCER

Consider an ensemble of  $N_k(t)$  cancer cell subpopulations (indexed by k); the total number of cancer cells is given by  $N(t) = \sum_k N_k(t)$ , and the PSA level is assumed to obey the following ordinary differential equation (ODE):

$$\frac{d}{dt} PSA(t) = \lambda N(t) - \Xi PSA(t) , \qquad (1)$$

where the PSA decay rate is  $\Xi \sim 3.5 \times 10^{-1}/\mathrm{day}$  (corresponding to a characteristic decay timescale of about a few days [18]) and  $\lambda$  is the PSA production rate per cell, assumed uniform across sub-populations. It is crucial to note that not all cancer cells produce PSA in the same way or at consistent levels over time; here we are relying on a rather simplistic assumption for such a complex disease to guide our estimation for parameters that describe cancer dynamics. Since the rate  $\Xi$  is significantly larger than the cancer cell growth rates (which ranges from  $2 \times 10^{-3}$  to  $2 \times 10^{-2}/\mathrm{day}$ , as estimated in [17]), we can further adopt the additional quasi-steady state approximation (QSA):

$$PSA(t) \approx (\lambda/\Xi) N(t) , \qquad (2)$$

meaning that the system is considered highly overdamped.

The oncologist (the "game leader"), begins somewhere in the game at an unknown point, presented with a patient showing elevated PSA levels, that is we do NOT know the carrying capacity of the patient's tumor. Let us consider a simplified version for the basic case of only two prostate cancer cell sub-populations under the influence of a single drug: (1) a drug-sensitive population  $N_S(t)$ , and (2) a drug-resistant population  $N_R(t)$ . In this model, we assume no treatment- or time-dependence to their phenotypes. That is, there is no de novo resistance evolution: no phenotype switching or mutagentic response in the cancer cells to hormone deprivation. Both cell phenotypes share a common cell carrying capacity K in the absence of treatment. The cancer dynamics is then described by the following two simple coupled ODEs [17]:

$$\frac{d}{dt}N_S(t) = r_S \left[ 1 - \left( \frac{N_S(t) + N_R(t)}{K \left[ 1 - \gamma \Lambda(t) \right]} \right) \right] N_S(t) ,$$

$$\frac{d}{dt}N_R(t) = r_R \left[ 1 - \left( \frac{N_R(t) + \alpha_{RS}N_S(t)}{K} \right) \right] N_R(t) ,$$
(3)

in which  $r_S, r_R > 0$  are maximum growth rates of sensitive and resistant cells; the cells compete for a resource (testosterone) with the competition coefficient  $\alpha_{RS} \geq 0$ . This coefficient

represent how the two cell types interact and affect each other indirectly through their distinct metabolisms and influence on the tumor microenvironment [19]. In Eq. (3), the effect of the drug is to reduce the carrying capacity for sensitive cells by a factor of  $\gamma\Lambda(t)$ , where  $\Lambda(t)$  denotes the time-dependent level of the drug administered to the patient. The value  $\gamma$  represents the drug effectiveness,  $0 \le \gamma \le 1$ . We take  $\Lambda(t)$  to be binary:  $\Lambda(t) = 0$  during periods of no drug administration, and  $\Lambda(t) = 1$  during periods of (maximum) dosage. The use of  $\gamma\Lambda(t)$  may appear ad-hoc, but it is predicated the presence of Abiraterone, which reduces the carrying capacity by a factor of  $(1 - \gamma)$  for only drug-sensitive T<sup>+</sup> populations, but stays unchanged for resistant T<sup>-</sup> populations.

Eq. (2) and Eq. (3) contain six parameters, i.e.  $\{r_S, r_R, \alpha_{RS}, \gamma, K, \lambda\}$ . Presumably all these parameters are patient-specific. In addition, there are at least two more unknowns, related to the *initial* cancer population sizes  $\{x_S(0), x_R(0)\}$  for each patient. It is important to note that at t = 0 for each patient, they have already received other treatments (e.g., chemical castration) in preparation for the study. The modeler must determine parameter values of each patient. In previous work by Zhang et al. [20], finding unique patient-specific parameters was not done systematically. Simulations were carried out assuming all patients entered the trial at roughly half of that value, guaranteeing that adaptive therapy would have a profound effect. This assumption of being close to carrying capacity in the simulations was carried forward into the clinical trials, where PSA levels were set to a normalized value of 1 for all patients to be near the carrying capacity. There was no attempt to actually determine carrying capacity from a dose-response experiment. In subsequent work by Zhang et al. [17], the parameters have been determined systematically but under an arbitrary choice for drug effectiveness and an assumption that the cancer growth rates are identical across patients, which is not supported by the data. Furthermore, the trigger points for on/off for abiraterone therapy were arbitrarily set (the PSA off-level is half that of the PSA on-level), with no attempt to optimize these values.

Hansen and Read et al. [16] realized that the Zhang et al. [17] lacked optimization. They pointed out that actually setting the off trigger close to the carrying capacity, and setting the on trig as close as possible to the one one actually could significantly improve patient time to progression, which of course makes sense since maintaining the  $T^+$  population at as high a value as possible within the confines of this simple model can only help suppress the  $T^-$  population. This was an imporpant advance, but unfortunately Hansen and Read

presented no systematic procedure for actually determining carrying capacity numbers from patient data. As they point out, if one starts far from the carrying capacity and with closely matched populations of  $T^+$  and  $T^-$  an adaptive protocol can actually suppress the  $T^+$  population and help the  $T^-$ , a disaster.

The only way to achieve a true patient specific model of that patient's disease state is through experimentation, i.e. administering brief doses of Abiraterone and measuring PSA levels over time to fit all the parameters to the measured PSA trajectories for each patient. Once parameters are established, the oncologist can use them to project the future of cancer progression for each patient in a Stackelberg game, and can even perform treatment optimization and open-loop planning. To begin, we need to make some assumptions to reduce the number of free parameters, ensuring that the fit remains predictive while avoiding excessive aggregating/simplification that could lead to an inaccurate prediction of cancer progression under treatment.

# III. A MORE DETAILED STACKELBERG GAME THEORY MODEL OF ADAPTIVE THERAPY FOR PROSTATE CANCER

A central problem in achieving a truly personal, patient-specific model for treating mCRPC is the large number of free parameters. For a patient with fewer than  $\sim 10$  PSA blood level measurements (typically, a patient in [17] has around  $\sim 20$  measurements), the parameters in the ODEs in Eq. (2) and Eq. (3) cannot be reliably identified when fitting observational data. We therefore now consider constraining these parameters while being careful not to arbitrarily fix too many of them.

For any individual patient, we can re-write the system of ODEs describing the evolution of the observable PSA level and the cancer progression, i.e. Eq. (2) and Eq. (3), as follows:

$$PSA(t) \approx \tilde{\lambda}x(t) ,$$

$$\frac{d}{dt}x_{S}(t) = r_{S} \left[ 1 - \left( \frac{x_{S}(t) + x_{R}(t)}{1 - \gamma \Lambda(t)} \right) \right] x_{S}(t) ,$$

$$\frac{d}{dt}x_{R}(t) = r_{R} \left[ 1 - \left( x_{R}(t) + \alpha_{RS}x_{S}(t) \right) \right] x_{R}(t) ,$$
(4)

in which  $x_S(t), x_R(t)$ , and  $x(t) \equiv x_S(t) + x_R(t)$  are the sensitive, resistant, and total cancer cell populations respectively, scaled by a common carrying capacity K:

$$x_S(t) \equiv N_S(t)/K$$
,  $x_R(t) \equiv N_R(t)/K$ . (5)

The quantity  $\tilde{\lambda} \equiv (\lambda/\Xi)K$  is the ratio of the PSA production rate to its decay rate when the cancer reaches its carrying capacity; this is also equal to the carrying capacity PSA measurement under QSA:

$$PSA_K \equiv PSA\Big|_{x=1} = \tilde{\lambda} . \tag{6}$$

It is important to note that cancer can cause symptoms, complications, and even become lethal before x(t) reaches 1.

Assuming that the above description is adequate across patients, then if the seven parameters  $\{\tilde{\lambda}, r_S, r_R, \alpha_{RS}, \gamma, x_S(0), x_R(0)\}$  are known for each and every patient, the PSA trajectories can be fully determined using Eq. (4) for any drug treatment schedule  $\Lambda(t)$ . Note that all of these parameters may differ between patients; however, by assuming some are common, we can still achieve a good fit for all patients and, most important, infer some general behavior of prostate cancer biophysics to guide and optimize treatments. Also, not all of these parameters are of equal importance. As we will discuss in Section V, the parameters that have the most influence on patient outcomes, when treatment is optimal, are the common ecological competition coefficient  $\alpha_{RS}$  and the patient-specific biomarker level at carrying capacity  $PSA_K = \tilde{\lambda}$ .

Consider the *relative* kinetics between sensitive and resistant cells to be universal across patients. This means that the growth and competition of sensitive and resistant cells are locally identical across patients, differing only by a timescale. We can thus further divide the seven parameters into two sets:

- The two common parameters  $\{r_S/r_R, \alpha_{RS}\}$ , representing the ratio between growth rates and the ecological competition coefficient.
- The five patient-specific parameters

$$\{\tilde{\lambda}, r_R, \gamma, x_S(0), x_R(0)\} , \qquad (7)$$

which are the PSA measurement when the cancer population reaches carrying capacity, the resistant cell growth rate, the drug effectiveness, and the initial populations sizes of the two different cancer cell phenotypes at the beginning of PSA tracking for each individual patient. This is the smallest set of parameters that should not be identical across patients.

In contrast to the previous study [17], here we acknowledge that cancer growth and patient responses to drug may vary drastically between individuals. These considerations are consistent with crude estimations of growth rates for a subset of patients [17] and with findings related to Abiraterone responses [21, 22]. We also did not fix any parameter values before fitting the model, as [17] did for  $\gamma = 90\%$  and  $r_S/r_R = 1.66$  [17]; instead, we obtain these values from the fitting procedure. Note that we did explore other options for both common parameters and patient-specific parameters, but the selection above appears to provide the best fit.

If the common parameters are known, early measurements of PSA(t) during on- and off-drug periods allow us to estimate the patient-specific parameters. These estimates can be updated and refined as additional data becomes available. We can then use Eq. (4) to predict future PSA(t) observations and the growth trajectories of the two cell types, sensitive  $x_S(t)$  and resistant  $x_R(t)$ , in response to different drug administration schedules.

The only explicitly time dependent term in Eq. 4 is  $\Lambda(t)$ , and it lies at the heart of the clinician strategy. In principle  $\Lambda(t)$  can be any function of time, yet, given the realities of delivering chemotherapy to patients, we assume that drug delivery is determined not directly by time but rather by trigger levels of measured PSA. That is, we allow only two knobs to tune: the on-level PSA<sub>↑</sub> and off-level PSA<sub>↓</sub>. In adaptive therapy, the drug is administered when the patient PSA level surpasses the on-level PSA<sub>↑</sub> and continues until it decreases to the off-level PSA<sub>↓</sub>. Drug administration is then resumed only when the PSA level returns to PSA<sub>↑</sub>.

The clinician goal is to prevent the patient from staying in a state of developing symptoms (e.g. as urinary issues, erectile dysfunction, pelvic pain, bone pain), which emerge when their prostate cancer have advanced far enough. We denote the PSA level at which symptoms begin to appear as  $PSA_{thr}$ , a value that is not known in advance. At that stage, drug administration cannot be delayed without risking further complications. For all patients in [17], Abiraterone was first administered to all patients well before any signs of symptoms appeared. We define the two policy parameters,  $\eta_{\uparrow}$  and  $\eta_{\downarrow}$ , so that  $PSA_{\uparrow}$  is a fraction  $\eta_{\uparrow}$  of the clinician acceptable upper limit  $PSA_{thr}$ , and  $PSA_{\downarrow}$  is a fraction  $\eta_{\downarrow}$  of  $PSA_{\uparrow}$ :

$$PSA_{\uparrow} \equiv \eta_{\uparrow} PSA_{thr} , PSA_{\downarrow} \equiv \eta_{\downarrow} PSA_{\uparrow} = \eta_{\uparrow} \eta_{\downarrow} PSA_{thr} .$$
 (8)

The values of  $\eta_{\uparrow}$  and  $\eta_{\downarrow}$  are therefore bounded between 0 and 1.

Given this formulation, patient-informed parameters and the PSA threshold value  $PSA_{thr}$ , we can now attempt to determine what the optimal treatment policy should be for the patient.

#### IV. PATIENT-INFORMED PARAMETER ESTIMATION

#### A. Clinical Data and Nonlinear Mixed Effect

We reanalyze the clinical data from [17], which includes N=32 patients undergoing Abiraterone treatment. Note that these patients have already received treatment to block male hormone production from the pituitary gland, which accounts for approximately  $\sim 90\%$ of total production. Abiraterone is used as an additional therapy, to inhibit androgen production from other sources, including the adrenal glands and the tumor itself, which contribute the remaining  $\sim 10\%$  of total production. Considerations in our analysis differ from those of [17] in certain direction:

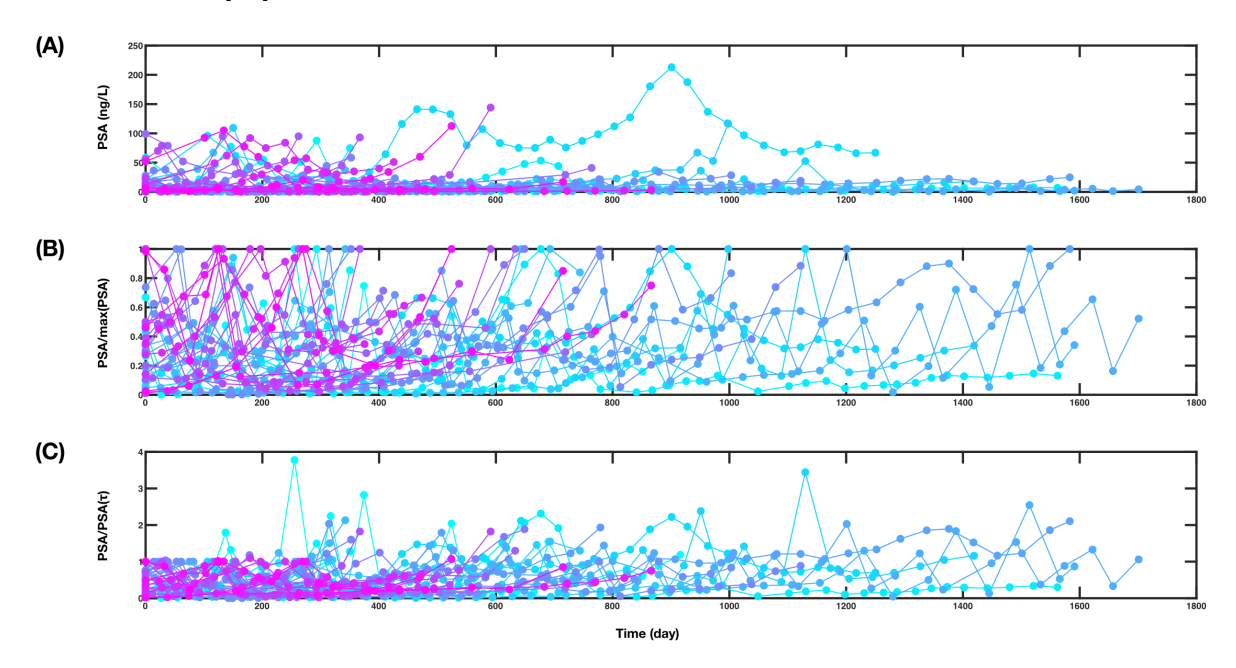


FIG. 1: Time series of PSA levels for all N=32 patients, for alternative normalizations. (A) The PSA level in ng/L. (B) The PSA level as normalized in Zhang et al. [17], in which the maximum value of any given PSA time series after the normalization is always at 1. (C) The normalized PSA level is adjusted so that the value at the start of the first treatment in any given PSA time series is always set to 1 after normalization.

• In Fig. 1A we show the raw time series data for the PSA level (in ng/L) of all patients.

It is very important to note that these data are widely different in scale (the maximum value in each of these PSA time series ranges from  $\sim 2 \text{ng/L}$  to  $\sim 200 \text{ng/L}$ ), so before fitting the model to all patients, we need to normalize them to ensure comparability between patients. If not, the fit will then be overly controlled by the highly volatile patients. Here, we normalize each patient's PSA measurement data using the PSA value at the time Abiraterone was first administered (see Fig. 1C), instead of the maximum PSA value as in [17] (see Fig. 1B). This choice for normalization not only still ensures comparability between PSA time series across all patients, but also allows for data updates without necessitating changes to previous entries.

- We decide to relax the assumption in [17] that the cancer growth rates  $r_S$  and  $r_R$  are identical for all patients. This is consistent with the values estimated for patients receiving continuous drug treatment, ranging from  $2 \times 10^{-3}$  to  $2 \times 10^{-2}/\text{day}$  [17]. Instead, we permit  $r_R$  to vary among patients while treating the ratio of these rates,  $r_S/r_R$ , as universal. We do not pre-set  $r_S/r_R$ .
- We let the drug effectiveness  $\gamma$  to be a free parameter instead of fixing it. This allows for variability in how different patients respond to the drug, and provides a more accurate assessment of how close the initial total cancer cell population is to the carrying capacity, i.e. how close x(0) is to 1.
- The model is nonlinear in both common as well as person specific (mixed) factors. For this reason, we utilize an established statistical approach, the empirical Bayes approach of Lindstrom and Bates [23], to fit the model to the normalized PSA data within the framework of nonlinear mixed effects (NLME). The estimated parameters for fitting the model to the data are selected so as to maximize the observation likelihood, meaning they provide the best possible explanation for the patterns seen in the data. Not only do we have estimates for the two common parameters  $\{\alpha_{RS}, r_S/r_R\}$ , we also obtain probability distributions for four patient-specific parameters

$$\{r_R, \gamma, x_S(0), x_R(0)\}\ .$$
 (9)

Estimation of the *patient-specific parameters* benefits from regarding them as samples from a distribution, since it statistically addresses the regression to the mean for extreme values.

• We do not assign weights differently (and rather arbitrarily) to different events (e.g. the first data points after a treatment change, from off-drug to on-drug and *vice versa*, are weighted five times more than the others in [17]). Here, all data points are treated the same.

Note that there are five patient-specific parameters as previously mentioned in Eq. (7), but Eq. (9) addresses only four: the fifth,  $\tilde{\lambda}$ , is determined by the other four.

To be more precise, let us denote the two common parameters as  $\Theta \equiv \{\alpha_{RS}, r_S/r_R\}$  and the four patient-specific parameters (besides  $\tilde{\lambda}$ ) as  $\theta \equiv \{\gamma, r_R, x_S(0), x_R(0)\}$ , and use the subscript  $\mu$  to specify the individual patient, i.e.  $\theta_{\mu}$ . For each patient  $\mu$  in [17], we know their given Abiraterone treatment schedule  $\Lambda_{\mu}(t)$ , and the measurement times  $t_{m_{\mu}}$  (where  $m_{\mu}$  labels the time point) at which they have their PSA level recorded, as well as the measured values  $PSA_{\mu}(t_{m_{\mu}})$ . If  $m_{\mu}^{\text{(treat)}}$  is the time point when Abiraterone was first administered, then the normalized PSA level can be calculated with:

$$\overline{\mathrm{PSA}}_{\mu}(t_{m_{\mu}}) = \mathrm{PSA}_{\mu}(t_{m_{\mu}})/\mathrm{PSA}_{\mu}(t_{m_{\mu}^{(\mathrm{treat})}}) . \tag{10}$$

For a given  $\{\Theta, \theta_{\mu}; \Lambda_{\mu}(t)\}$ , we can use Eq. (4) to obtain theoretically what trajectory the total cancer cell population should be,<sup>1</sup> which we denote as  $x^{\{\Theta,\theta_{\mu};\Lambda_{\mu}(t)\}}(t)$ . The theoretical trajectory for the *normalized* PSA level, therefore, follows from Eq. (4) if  $\tilde{\lambda}_{\mu}$  is known:

$$\overline{\mathrm{PSA}}^{\{\Theta,\theta_{\mu};\Lambda_{\mu}(t)\}}(t) = \tilde{\lambda}_{\mu} x^{\{\Theta,\theta_{\mu};\Lambda_{\mu}(t)\}}(t) / \mathrm{PSA}_{\mu}(t_{m_{\mu}^{(\mathrm{treat})}}) . \tag{11}$$

We then estimate  $\tilde{\lambda}_{\mu}$  by minimizing the sum squared-errors (SSE) between the observational  $\overline{\text{PSA}}_{\mu}(t_{m_{\mu}})$  and the theoretical  $\overline{\text{PSA}}^{\{\Theta,\theta_{\mu};\Lambda_{\mu}(t)\}}(t_{m_{\mu}})$ :

$$\tilde{\lambda}_{\mu} = \arg \min \left\{ \sum_{m_{\mu}}^{\text{given } \mu} \left[ \overline{PSA}_{\mu}(t_{m_{\mu}}) - \overline{PSA}^{\{\Theta,\theta_{\mu};\Lambda_{\mu}(t)\}}(t_{m_{\mu}}) \right]^{2} \right\}$$

$$= \frac{\sum_{m_{\mu}}^{\text{given } \mu} \overline{PSA}_{\mu}(t_{m_{\mu}}) x^{\{\Theta,\theta_{\mu};\Lambda_{\mu}(t)\}}(t_{m_{\mu}})}{\sum_{m_{\mu}}^{\text{given } \mu} \left[ x^{\{\Theta,\theta_{\mu};\Lambda_{\mu}(t)\}}(t_{m_{\mu}}) \right]^{2}} = \frac{\sum_{m_{\mu}}^{\text{given } \mu} PSA_{\mu}(t_{m_{\mu}}) x^{\{\Theta,\theta_{\mu};\Lambda_{\mu}(t)\}}(t_{m_{\mu}})}{\sum_{m_{\mu}}^{\text{given } \mu} \left[ x^{\{\Theta,\theta_{\mu};\Lambda_{\mu}(t)\}}(t_{m_{\mu}}) \right]^{2}} . \tag{12}$$

In other words,  $\lambda_{\mu}$  is determined by  $\{\Theta, \theta_{\mu}; \Lambda_{\mu}(t)\}$  and the time series  $PSA_{\mu}(t_{m_{\mu}})$  for each individual patient  $\mu$ .

 $<sup>^{1}</sup>$  We employ the fourth-order Runge-Kutta method for numerical integration to derive the trajectory in MatLab R2023a [24].

#### B. Statistical Assumptions

To use the Lindstrom-Bates empirical Bayes (LBEB) approach for NLME [23], we need to make some statistical assumptions:

• The discrepancies in the data fit are sampled from a combined-variance Gaussian noise, which includes both a constant component and a component that is proportional to the "true" value. This means that measurements for a larger "true" value are allowed to exhibit greater variability, i.e.:

$$\overline{\text{PSA}}_{\mu}(t_{m_{\mu}}) = \overline{\text{PSA}}^{\{\Theta,\theta_{\mu},\Lambda_{\mu}(t)\}}(t_{m_{\mu}}) + \eta_{\mu}(t_{m_{\mu}}) , \qquad (13)$$

where the errors  $\eta_{\mu}(t_{m_{\mu}})$  are sampled from a Gaussian distribution:

$$\left[A + B \ \overline{\mathrm{PSA}}^{\{\Theta,\theta_{\mu};\Lambda_{\mu}(t)\}}(t_{m_{\mu}})\right] \mathcal{N}(0,1) \ . \tag{14}$$

Here A, B are two unknown positive constants, and  $\mathcal{N}(0,1)$  represents the Gaussian distribution centered at 0 with a variance of 1.

• The four patient-specific parameters  $\{r_R, (1-\gamma), x_S(0), x_R(0)\}$  are assumed to be sampled from four log-normal distributions [25]. Note that we consider  $(1-\gamma)$  to be sampled from a log-normal distribution, not  $\gamma$ , because observations (PSA levels before and after Abiraterone administration) suggest that  $\gamma$  is typically much closer to 1 than 0.

We then apply the LBEB approach<sup>2</sup> to estimate the common parameters  $\{r_S/r_R, \alpha_{RS}\}$ , the log-normal distributions of  $\{r_R, (1-\gamma), x_S(0), x_R(0)\}$ , and the values  $\{r_R, \gamma, x_S(0), x_R(0)\}$  of each patient, and also the two constants A, B that characterized our noise function, so that the observations across patients can be the most likely ones (maximum likelihood).

#### C. Best-Fit Results

We start by acknowledging that the clinical data is extremely noisy, which should be expected. The fit found in Zhang et al. [17], while not quantitative, does capture nearly all

 $<sup>^2</sup>$  We use the standard package nlmefit in MatLab R2023a [24] to algorithmically execute LBEB approach for NLME.

the qualitative behavior of every patients regarding PSA response on- and off-drug. However, the total SSE for all patients of this fit is very large, which motivates us to reanalyze their data. While we still consider two common parameters, we now use four patient-specific parameters instead of only two, resulting in a significantly better fit, as shown in Fig. 2 and Fig. 3. The total SSE has been reduced by more than a factor of three, from 170.68 for Zhang et al. [17] fit to 57.52 for our LBEB approach. The SSE for individual patients is also typically smaller using our approach (26 out of 32).

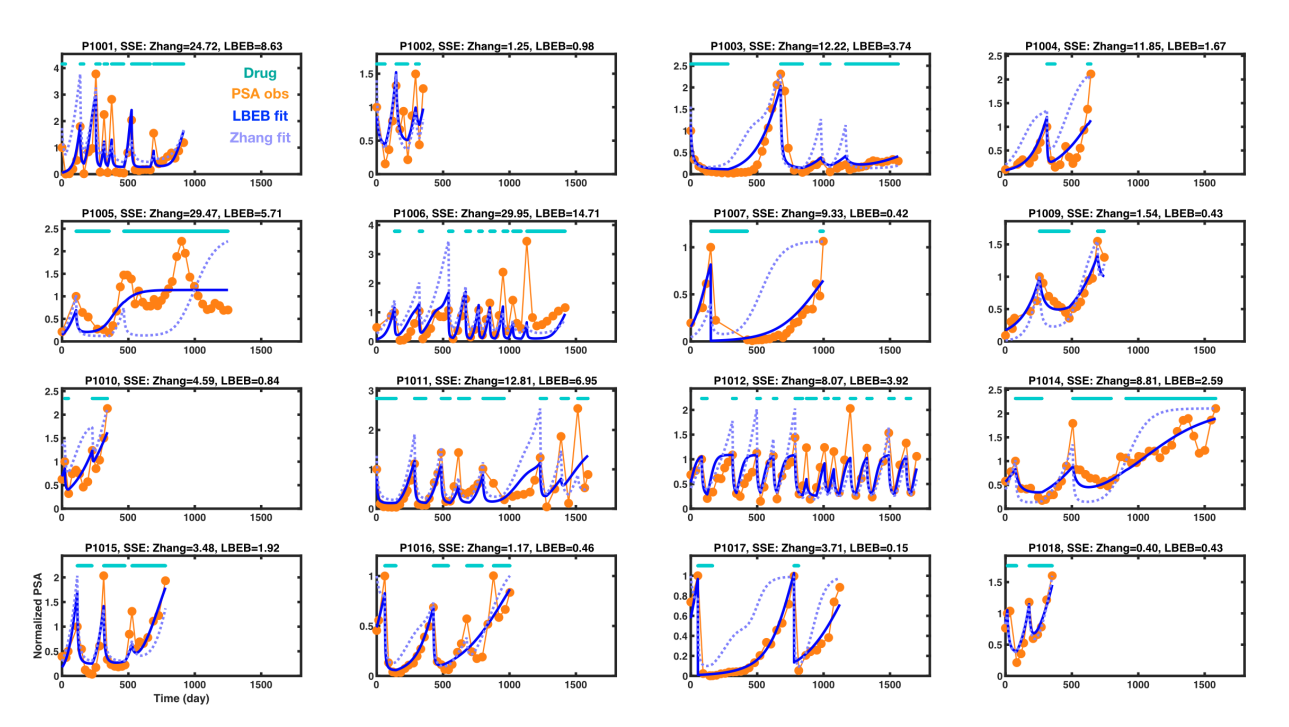


FIG. 2: Time series of PSA levels for the first 16 patients. Each plot title shows the patient's name, SSE for Zhang et al. [17] fit, and the LBEB fit. The cyan line marks drug use periods, orange dots represent normalized PSA Eq. (10), the light-blue dashed line shows Zhang et al. [17] best fit, and the blue line shows the LBEB best fit.

We find the best common parameter values to be  $r_S/r_R = 2.97 \pm 0.02$  and  $\alpha_{RS} = 5.2 \pm 0.9$ . This provides strong evidence that  $r_S > r_R$ . The large value for the competition coefficient  $\alpha_{RS}$  between resistant and sensitive cells agrees with the findings of [17], indicating the robustness of this estimation even with different approaches. The patient-specific parameters are sampled from

$$r_R \sim (7.0 \times 10^{-3}) \exp \left[0.7 \,\mathcal{N}(0,1)\right] \;,\; \gamma \sim 1 - (4.0 \times 10^{-2}) \exp \left[1.5 \,\mathcal{N}(0,1)\right] \;,$$
  $x_S(0) \sim (4.1 \times 10^{-2}) \exp \left[2.4 \,\mathcal{N}(0,1)\right] \;,\; x_R(0) \sim (2.3 \times 10^{-2}) \exp \left[1.8 \,\mathcal{N}(0,1)\right] \;.$ 

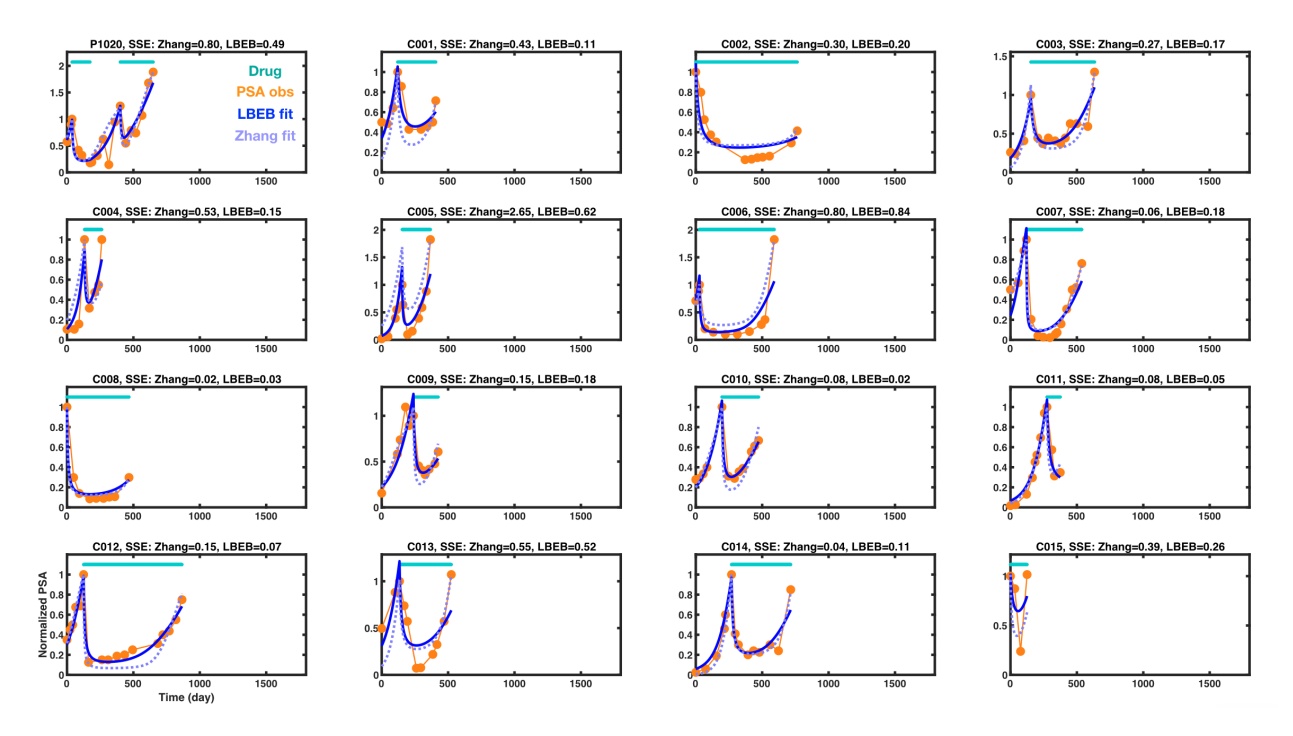


FIG. 3: Time series of PSA levels for the next 16 patients. Each plot title shows the patient's name, SSE for Zhang et al. [17] fit, and the LBEB fit. The cyan line marks drug use periods, orange dots represent normalized PSA Eq. (10), the light-blue dashed line shows Zhang et al. [17] best fit, and the blue line shows the LBEB best fit.

We report the individual values for the patient-specific parameters in Appendix A. Fig. 4A shows a slight positive trend (presented in log-log plot) between the resistant cell growth rate  $r_R$  and the drug ineffectiveness  $1 - \gamma$ . This indicates that in patients where cancer cells can multiply quickly and thrive, Abiraterone is usually less effective in suppressing the disease. Fig. 4B reveals that, initially before treatment, sensitive cells contribute the most to prohibiting the growth of resistant cells (compared to resistant cells themselves). We show the monotonic relationship between the PSA level at the time of first drug treatment, PSA( $t_{m^{\text{treat}}}$ ), and the PSA level at carrying capacity, PSA<sub>K</sub>, in Fig. 4C. For 27 out of the total N=32 patients, PSA( $t_{m^{\text{treat}}}$ )/PSA<sub>K</sub> >  $1/\alpha_{RS}$ , which carries significant clinical implications that we will discuss in Section V B.

#### D. Comparison between Models

It should, of course, be expected that with more free parameters we should achieve better a fit. Therefore, we need to assess whether the improved fit justifies the additional parameters and helps avoid overfitting, ensuring that the model will perform well on new

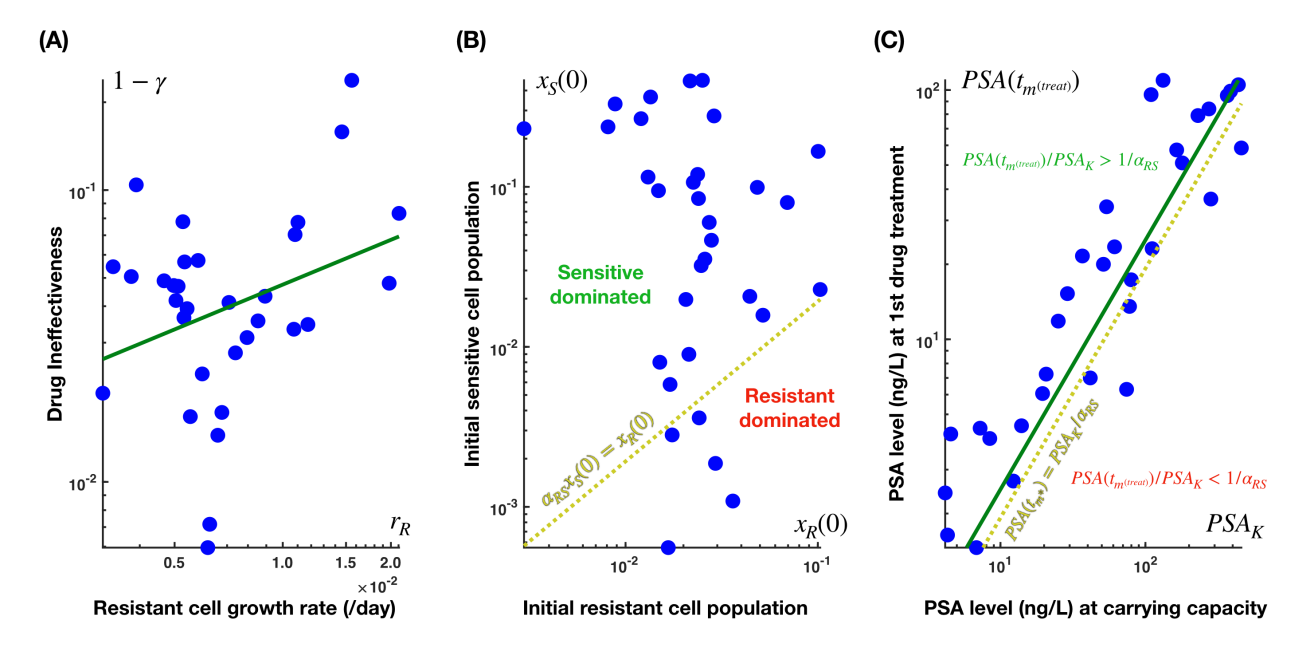


FIG. 4: The relations between patient-specific parameters and the PSA level at the first drug treatment. Here we show the identified resistant cell growth rate  $r_R$ , drug effectiveness  $\gamma$ , and initial population values  $\{x_S(0), x_R(0)\}$ , and the PSA level when the total cancel population reaches its carrying capacity  $PSA_K = \tilde{\lambda}$  for all patients. (A) The resistant cell growth rate  $r_R$  and the drug ineffectiveness  $1-\gamma$ . The green continuous line shows a slight positive trend between these parameters in log-log plot  $(R^2 = 0.10 \ [26])$ , indicating a power-law relation  $1-\gamma \propto r_R^{0.5\pm0.5}$ . (B) The initial values  $\{x_S(0), x_R(0)\}$ . The yellow dash line divides this two-dimensional parameter space into two: sensitive cell dominated (above) and resistant cell dominated (below), based on their influences on the growth of resistant cells at t=0. (C) The PSA levels at first drug treatment  $PSA(t_{m^{treat}})$  and at carrying capacity  $PSA_K$ . The green continuous line shows a linear regression (that passes through the origin) between these parameters  $(R^2 = 0.59 \ [26])$ , indicating a linear relation  $PSA(t_{m^{treat}}) = (0.25\pm0.05) PSA_K$ . The yellow dash line divides this two-dimensional space into two:  $PSA(t_{m^{treat}})/PSA_K > 1/\alpha_{RS}$  (above) and  $PSA(t_{m^{treat}})/PSA_K < 1/\alpha_{RS}$  (below).

data.

For linear regression, the standard metric for "goodness-of-fit" is given by the  $R^2$ -value [26]. A direct generalization of this dimensionless metric for nonlinear models [27, 28] is commonly referred to as the Efron's pseudo- $R^2$ -value [29], is given by  $\tilde{R}^2 = 1 - \tilde{A}$ . The coefficient of alienation  $\tilde{A}$ , defined as [28]:

$$\tilde{A} = \frac{\text{SSE}}{\text{SS}_{\text{data}}} \ge 0 , \qquad (15)$$

where  $SS_{data}$  is the data variance (i.e. SSE with respect to the mean value). This measures the proportion of residual variation in the nonlinear model compared to a null model with no explanatory power, indicating how much the model deviates from an ideal fit. An ideal fit corresponds to  $\tilde{R}^2 = 1$ . While there are many other different proposals for goodness-of-fit depending on the specific characteristics of the nonlinear model being used [30–32], the Efron's pseudo- $\tilde{R}^2$ -value remains a useful metric due to its simplicity and ease of interpretation [28].

Since the number of parameters in the fit models that we use are not the same, i.e.  $n_{params} = (2 \times N) + 2 = 66$  in Zhang et al. [17] and  $n_{params} = (4 \times N) + 2 = 130$  in our approach, we need to calculate the *adjusted* Efron's psuedo- $R^2$ -value [33] instead:

$$\tilde{R}_{adj}^2 = 1 - \frac{\text{SSE}/(n_{\text{data}} - n_{\text{params}})}{\text{SS}_{\text{data}}/(n_{\text{data}} - 1)} . \tag{16}$$

We have  $n_{\text{data}} = 678$  and  $\text{SS}_{\text{data}} = 176.16$ . The closer  $\tilde{R}_{adj}^2$  is to 1, the more we can trust a fitted model. We obtain  $\tilde{R}_{adj}^2 \approx -0.08$  for Zhang et al. [17] fit and  $\tilde{R}_{adj}^2 \approx 0.60$  for our LBEB fit, which corroborates our approach.

#### V. OPTIMIZATION OF TREATMENT WITH ABIRATERONE

Within our adaptive therapy policy framework, our goal is to determine the optimal policy parameters  $(\eta_{\uparrow}, \eta_{\downarrow})$  that maximize the total achievable time  $\tau_{\text{tot}}$  we can keep the cancer progression (with treatment) below the biomarker level PSA<sub>thr</sub>, the level at which the patient begins to show symptoms, in order to avoid further complications. Consider the patients with two common parameters  $\Theta = \{r_S/r_R, \alpha_{RS}\}$  and the five patient-specific parameters  $\{\text{PSA}_K, \theta\} = \{\tilde{\lambda}, r_R, \gamma, x_S(0), x_R(0)\}$ , as found according to Section IV C. Note that  $\text{PSA}_K = \tilde{\lambda}$  follows, as explained in Eq. (6). For simplification, we further assume that the PSA level is measured continuously, and that there is no noise in these measurements, so that the decision to turn on and off drug treatment based on the policy parameters as described in Eq. (8) is exact. Hence, we can calculate the total achievable time  $\tau_{\text{tot}}$  below PSA<sub>thr</sub> using policy parameters  $(\eta_{\uparrow}, \eta_{\downarrow})$  for a patient  $\mu$  with parameters  $\{\Theta, \text{PSA}_{K\mu}, \theta_{\mu}\}$ , and we denote its full functional form as  $\tau_{\text{tot}}^{\{\Theta, \text{PSA}_{K\mu}, \theta_{\mu}\}, \text{PSA}_{\text{thr}}}(\eta_{\uparrow}, \eta_{\downarrow})$ . We can simplify this expression to  $\tau_{\text{tot}}^{\{\mu\}, \text{PSA}_{\text{thr}}}(\eta_{\uparrow}, \eta_{\downarrow})$ , and further drop all superscripts when it is clear which patient and what threshold are referred to.

As we will show in this Section through computer-assisted modeling, if the PSA threshold is too low  $PSA_{thr} \leq PSA_{K\mu}/\alpha_{RS}$  (remember that  $1/\alpha_{RS} \approx 0.19$ ), then for any policy parameters  $(\eta_{\uparrow}, \eta_{\downarrow})$ , the treatment appears to eventually fail, i.e. hence we can only hope to  $\frac{1}{3}$  We utilize the standard integrator ode23 in MatLab R2023a [24] to simulate Eq. (4) and implement the terminal condition, obtaining the total achievable time  $\tau_{tot}$  at when the simulated PSA level crosses the threshold value PSA<sub>thr</sub>.

somewhat prolong the drug response total achievable time  $\tau_{\text{tot}}$ . However, if this threshold is just high enough  $PSA_{\text{thr}} > PSA_{K\mu}/\alpha_{RS}$ , then sometimes, but not always, it is possible to find a treatment policy that arrests the cancer progression indefinitely  $\tau_{\text{tot}} \to \infty$ . We provide some analytical explanation for these possibilities in Section B.

A. 
$$PSA_{thr}/PSA_{Ku} \leq 1/\alpha_{RS}$$

Here, we search for the (global) maximum of the total achievable time (with treatment) below the PSA threshold,  $\tau_{\text{tot}}^{\{\mu\},\text{PSA}_{\text{thr}}}(\eta_{\uparrow},\eta_{\downarrow})$  over this multi-dimensional space  $(\eta_{\uparrow},\eta_{\downarrow})$ . We employ a Bayesian optimization approach [34] to efficiently navigate through the policy parameter space by data-driven extrapolation (kriging [35]) for the two-dimensional landscape  $\tau_{\text{tot}}^{\{\mu\},\text{PSA}_{\text{thr}}}(\eta_{\uparrow},\eta_{\downarrow})$  for patient  $\mu$  with a given PSA<sub>thr</sub>. This method, when applied to an objective function to be extremize, begins by evaluating that function at a number of random positions so as to (approximately) gauge its global features (using a surrogate model e.g. a Gaussian process [36]). It then uses Bayesian inference to predict the optimal next function evaluation location, balancing exploitation and exploration, and evaluate the function there. This iterative step continuously updates its estimation of the function, keeps finding and checking new locations and corresponding values, until the difference between two consecutive locations becomes sufficiently small (for a practical resolution of the parameter space).

#### 1. Bayesian Optimization

We briefly explain how we perform the computation for our optimal policy parameters

$$(\eta_{\uparrow}^*, \eta_{\downarrow}^*) = \arg\max \left[ \tau_{\text{tot}}^{\{\mu\}, \text{PSA}_{\text{thr}}} (\eta_{\uparrow}, \eta_{\downarrow}) \right] , \qquad (17)$$

using Bayesian optimization [34] with Gaussian process regression (GPR) [36]. Consider a search within the region  $(\eta_{\uparrow}, \eta_{\downarrow}) \in [0, 0.90] \times [0, 0.90]$ , where the resolution in each direction is  $\delta \eta = 0.01$ . Note that the upper bounds for  $\eta_{\uparrow}$  and  $\eta_{\downarrow}$  are both set at 0.90 instead of 1.00, as smaller differences (less that 10%) are clinically difficult to monitor [16]. We start by choosing  $n_{\text{eval}} = 10$  random points

$$\left\{(\eta_{\uparrow}^{(1)},\eta_{\downarrow}^{(1)}),(\eta_{\uparrow}^{(2)},\eta_{\downarrow}^{(2)}),...,(\eta_{\uparrow}^{(n_{\mathrm{eval}})},\eta_{\downarrow}^{(n_{\mathrm{eval}})})\right\}$$

within the search range of  $(\eta_{\uparrow}, \eta_{\downarrow})$ , and each point is assessed to determine the value of the total achievable time  $\tau_{\text{tot}}^{\{\mu\}, \text{PSA}_{\text{thr}}}(\eta_{\uparrow}, \eta_{\downarrow})$ . Using these initial evaluations, we then employ GPR to create a probabilistic extrapolation of  $\tau_{\text{tot}}^{\{\mu\}, \text{PSA}_{\text{thr}}}(\eta_{\uparrow}, \eta_{\downarrow})$  from the set of known values

$$\left\{\tau_{\mathrm{tot}}^{\{\mu\},\mathrm{PSA}_{\mathrm{thr}}}(\eta_{\uparrow}^{(1)},\eta_{\downarrow}^{(1)}),\tau_{\mathrm{tot}}^{\{\mu\},\mathrm{PSA}_{\mathrm{thr}}}(\eta_{\uparrow}^{(2)},\eta_{\downarrow}^{(2)}),...,\tau_{\mathrm{tot}}^{\{\mu\},\mathrm{PSA}_{\mathrm{thr}}}(\eta_{\uparrow}^{(n_{\mathrm{eval}})},\eta_{\downarrow}^{(n_{\mathrm{eval}})})\right\}\ .$$

This set provides not only an estimation

$$\hat{\tau}_{\mathrm{tot}}^{\{\mu\},\mathrm{PSA}_{\mathrm{thr}};\left\{(\eta_{\uparrow}^{(1)},\eta_{\downarrow}^{(1)}),(\eta_{\uparrow}^{(2)},\eta_{\downarrow}^{(2)}),...,(\eta_{\uparrow}^{(n_{\mathrm{eval}})},\eta_{\downarrow}^{(n_{\mathrm{eval}})})\right\}}\left(\eta_{\uparrow},\eta_{\downarrow}\right)}$$

for the *total achievable time* at any untested point, but also quantifies the uncertainty of this estimation, i.e. the standard deviation

$$\hat{\sigma}_{\hat{\tau}_{\rm tot}}^{\{\mu\},{\rm PSA}_{\rm thr};\left\{(\eta_{\uparrow}^{(1)},\eta_{\downarrow}^{(1)}),(\eta_{\uparrow}^{(2)},\eta_{\downarrow}^{(2)}),...,(\eta_{\uparrow}^{(n_{\rm eval})},\eta_{\downarrow}^{(n_{\rm eval})})\right\}}\!\!\left(\eta_{\uparrow},\eta_{\downarrow}\right)\;.$$

Bayesian optimization utilize this GPR extrapolation<sup>4</sup> to identify the next candidate points in the search space,  $(\eta_{\uparrow}^{(n_{\text{eval}}+1)}, \eta_{\downarrow}^{(n_{\text{eval}}+1)})$ , where the *total achievable time* is likely to be maximized with some confidence. This is done by balancing exploration (searching in regions with high uncertainty) and exploitation (focusing on regions predicted to have high values):

$$(\eta_{\uparrow}^{(n_{\text{eval}}+1)}, \eta_{\downarrow}^{(n_{\text{eval}}+1)}) = \arg\max \left[ \hat{\tau}_{\text{tot}}^{\{\mu\}, \text{PSA}_{\text{thr}}; \left\{ (\eta_{\uparrow}^{(1)}, \eta_{\downarrow}^{(1)}), (\eta_{\uparrow}^{(2)}, \eta_{\downarrow}^{(2)}), \dots, (\eta_{\uparrow}^{(n_{\text{eval}})}, \eta_{\downarrow}^{(n_{\text{eval}})}) \right\}} (\eta_{\uparrow}, \eta_{\downarrow}) \right.$$

$$\left. + \chi \hat{\sigma}_{\hat{\tau}_{\text{tot}}}^{\{\mu\}, \text{PSA}_{\text{thr}}; \left\{ (\eta_{\uparrow}^{(1)}, \eta_{\downarrow}^{(1)}), (\eta_{\uparrow}^{(2)}, \eta_{\downarrow}^{(2)}), \dots, (\eta_{\uparrow}^{(n_{\text{eval}})}, \eta_{\downarrow}^{(n_{\text{eval}})}) \right\}} (\eta_{\uparrow}, \eta_{\downarrow}) \right] .$$

$$(18)$$

We consider  $\chi = 2$ , corresponding to  $\approx 95\%$  confidence. We then update the extrapolation and repeat the above procedure for subsequent iterations, i.e.  $n \ge n_{\rm eval}$ :

$$\hat{\tau}_{\text{tot}}^{\{\mu\},\text{PSA}_{\text{thr}};\left\{(\eta_{\uparrow}^{(1)},\eta_{\downarrow}^{(1)}),(\eta_{\uparrow}^{(2)},\eta_{\downarrow}^{(2)}),\dots,(\eta_{\uparrow}^{(n)},\eta_{\downarrow}^{(n)})\right\}} (\eta_{\uparrow},\eta_{\downarrow}) 
\longrightarrow \hat{\tau}_{\text{tot}}^{\{\mu\},\text{PSA}_{\text{thr}};\left\{(\eta_{\uparrow}^{(1)},\eta_{\downarrow}^{(1)}),(\eta_{\uparrow}^{(2)},\eta_{\downarrow}^{(2)}),\dots,(\eta_{\uparrow}^{(n+1)},\eta_{\downarrow}^{(n+1)})\right\}} (\eta_{\uparrow},\eta_{\downarrow}) ,$$
(19)

$$\hat{\sigma}_{\hat{\tau}_{\text{tot}}}^{\{\mu\}, \text{PSA}_{\text{thr}}; \left\{ (\eta_{\uparrow}^{(1)}, \eta_{\downarrow}^{(1)}), (\eta_{\uparrow}^{(2)}, \eta_{\downarrow}^{(2)}), \dots, (\eta_{\uparrow}^{(n)}, \eta_{\downarrow}^{(n)}) \right\}} (\eta_{\uparrow}, \eta_{\downarrow}) 
\longrightarrow \hat{\sigma}_{\hat{\tau}_{\text{tot}}}^{\{\mu\}, \text{PSA}_{\text{thr}}; \left\{ (\eta_{\uparrow}^{(1)}, \eta_{\downarrow}^{(1)}), (\eta_{\uparrow}^{(2)}, \eta_{\downarrow}^{(2)}), \dots, (\eta_{\uparrow}^{(n+1)}, \eta_{\downarrow}^{(n+1)}) \right\}} (\eta_{\uparrow}, \eta_{\downarrow}) ;$$
(20)

<sup>&</sup>lt;sup>4</sup> We utilize the function *fitrgp* in MatLab R2023a [24] for this task, using the *ardmatern32* kernel function and the "exact fitting" option.

we then calculate:

$$(\eta_{\uparrow}^{(n+2)}, \eta_{\downarrow}^{(n+2)}) = \arg\max \left[ \hat{\tau}_{\text{tot}}^{\{\mu\}, \text{PSA}_{\text{thr}}; \left\{ (\eta_{\uparrow}^{(1)}, \eta_{\downarrow}^{(1)}), (\eta_{\uparrow}^{(2)}, \eta_{\downarrow}^{(2)}), \dots, (\eta_{\uparrow}^{(n+1)}, \eta_{\downarrow}^{(n+1)}) \right\}} (\eta_{\uparrow}, \eta_{\downarrow}) \right.$$

$$\left. + \chi \hat{\sigma}_{\hat{\tau}_{\text{tot}}}^{\{\mu\}, \text{PSA}_{\text{thr}}; \left\{ (\eta_{\uparrow}^{(1)}, \eta_{\downarrow}^{(1)}), (\eta_{\uparrow}^{(2)}, \eta_{\downarrow}^{(2)}), \dots, (\eta_{\uparrow}^{(n+1)}, \eta_{\downarrow}^{(n+1)}) \right\}} (\eta_{\uparrow}, \eta_{\downarrow}) \right] .$$

$$(21)$$

This iterative refinement continues until satisfactory convergence is achieved (which is chosen based on the resolution  $\delta \eta = 0.01$ ), and the final iteration gives an estimated value for  $(\eta_{\uparrow}^*, \eta_{\downarrow}^*)$  as the discovered global maximum of  $\tau_{\text{tot}}^{\{\mu\}, \text{PSA}_{\text{thr}}}(\eta_{\uparrow}, \eta_{\downarrow})$  along with the associated uncertainty.

#### 2. Optimal Treatment for Maximum $\tau_{tot}$

The optimization described in Section V A 1 can be applied to any patient; however, for illustrative purposes, we will consider patient P1007 as labelled in Fig. 2. This patient has small values for  $x_S(0)$  and  $x_R(0)$ , with  $x_S(0) \gg x_R(0)$ , allowing them to undergo several drug treatment cycles. We investigate  $\tau_{\text{tot}}(\eta_{\uparrow}, \eta_{\downarrow})$  for PSA<sub>thr</sub>/PSA<sub>K</sub> = 0.14 and 0.19. Fig. 5 shows the GPR extrapolated surface functions

$$\hat{\tau}_{\text{tot}}^{\{\mu\},\text{PSA}_{\text{thr}};\left\{(\eta_{\uparrow}^{(1)},\eta_{\downarrow}^{(1)}),(\eta_{\uparrow}^{(2)},\eta_{\downarrow}^{(2)}),\dots,(\eta_{\uparrow}^{*},\eta_{\downarrow}^{*})\right\}}(\eta_{\uparrow},\eta_{\downarrow})}$$
(22)

for these different PSA thresholds, i.e.  $PSA_{thr}/PSA_K = 0.14$  in Fig. 5A and  $PSA_{thr}/PSA_K = 0.19$  in Fig. 5B. The optimal policy parameter values  $(\eta_{\uparrow}^*, \eta_{\downarrow}^*)$  is located at the corner (0.90, 0.90), corresponding to the *highest possible on*-drug PSA level with the *tightest control*  $(\eta_{\downarrow})$  is maximum). We will see that this is consistent with our analytical considerations in Section B.

Fig. 6 shows our numerical findings for simulated treatments on this patient, using different policy parameters:

- Panel (A,D): Cancer progression under continuous Abiraterone treatment often results in resistant cells rapidly overtaking the population, causing the cancer to exceed the thresholds faster. Note that continuous therapy is a special case of adaptive therapy in which the off-drug policy parameter  $\eta_{\downarrow}$  is set to 0.
- Panel (B,E): Cancer progression under a (non-optimal) adaptive Abiraterone treatment, in which PSA<sub>↑</sub> is as high as possible and PSA<sub>↓</sub> is set to 50% of PSA<sub>↑</sub>. This

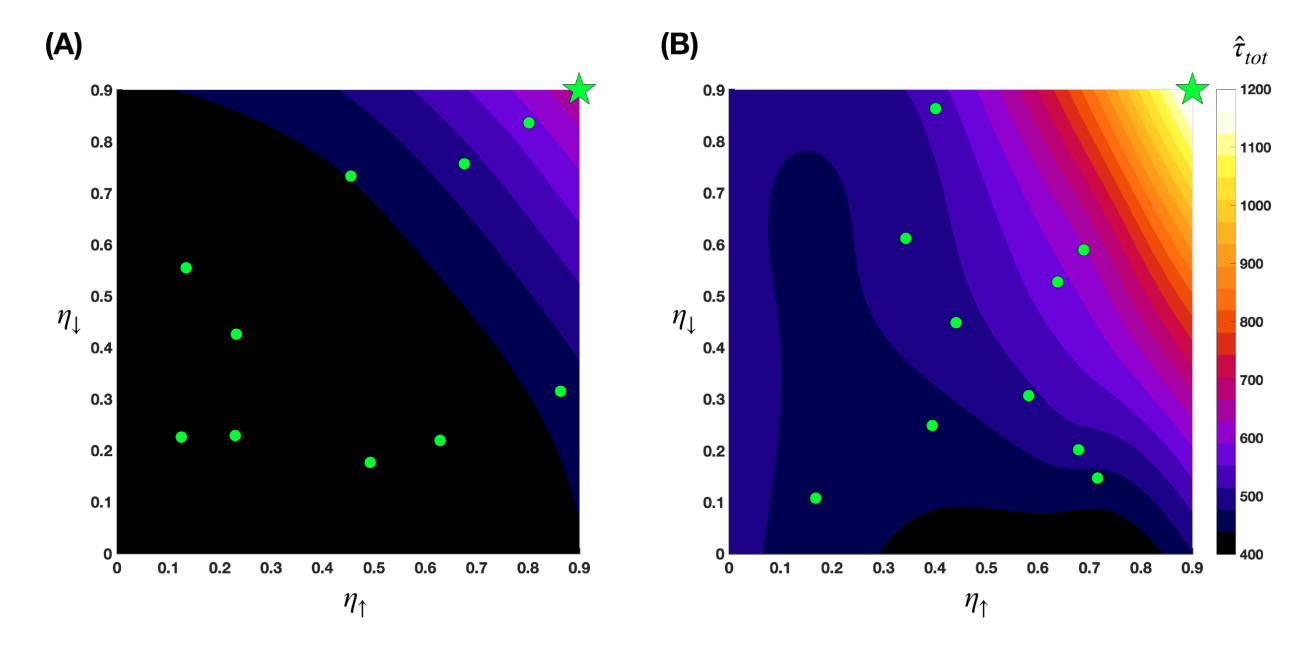


FIG. 5: Bayesian optimization using a GPR model to search for the maximum total drug response time  $\tau_{\text{tot}}$  for patient P1007 under adaptive chemotherapy. We consider different PSA threshold values, i.e.  $PSA_{\text{thr}}/PSA_K = 0.14$  in (A) and  $PSA_{\text{thr}}/PSA_K = 0.19$ . Here we show the Gaussian extrapolated surfaces of the total achievable time, as given in Eq. (22). The circles represent the points where the total achievable time is evaluated by numerical simulation. The star indicates the point of convergence for the search, which corresponds to the global maxmimum.

treatment has been used in studies and clinical trials [17]. Since the drug is not used to suppress sensitive cells constantly, these cells are allowed to recover and keep competing with the resistant ones longer, hence the *total achievable time* is extended.

• Panel (C,F): Cancer progression under the optimal adaptive treatment, found from Bayesian optimization. This suggests that, the closer the PSA level at which the patient starts showing symptoms  $PSA_{thr}$  is to  $PSA_K/\alpha_{RS}$  (which is rather far from when the cancer population may reach carrying capacity, since  $\alpha_{RS} \gg 1$ ), the more effective optimal adaptive therapy can be in prolonging the time gained compared to continuous treatment.

We observe in Fig. 5 that the most effective adaptive therapies maintain tight control of PSA levels with the highest on-drug PSA level, i.e.  $\eta_{\downarrow}, \eta_{\uparrow} \to 1$ , a strategy we refer to as high level tight control (HLTC). This treatment cycle involves administering Abiraterone in short bursts, followed by extended resting periods, at a high frequency. We report our found optimal policy parameters  $(\eta_{\uparrow}^*, \eta_{\downarrow}^*)$  for all patients with  $x(0) < \text{PSA}_{\text{thr}}/\text{PSA}_K$  in the

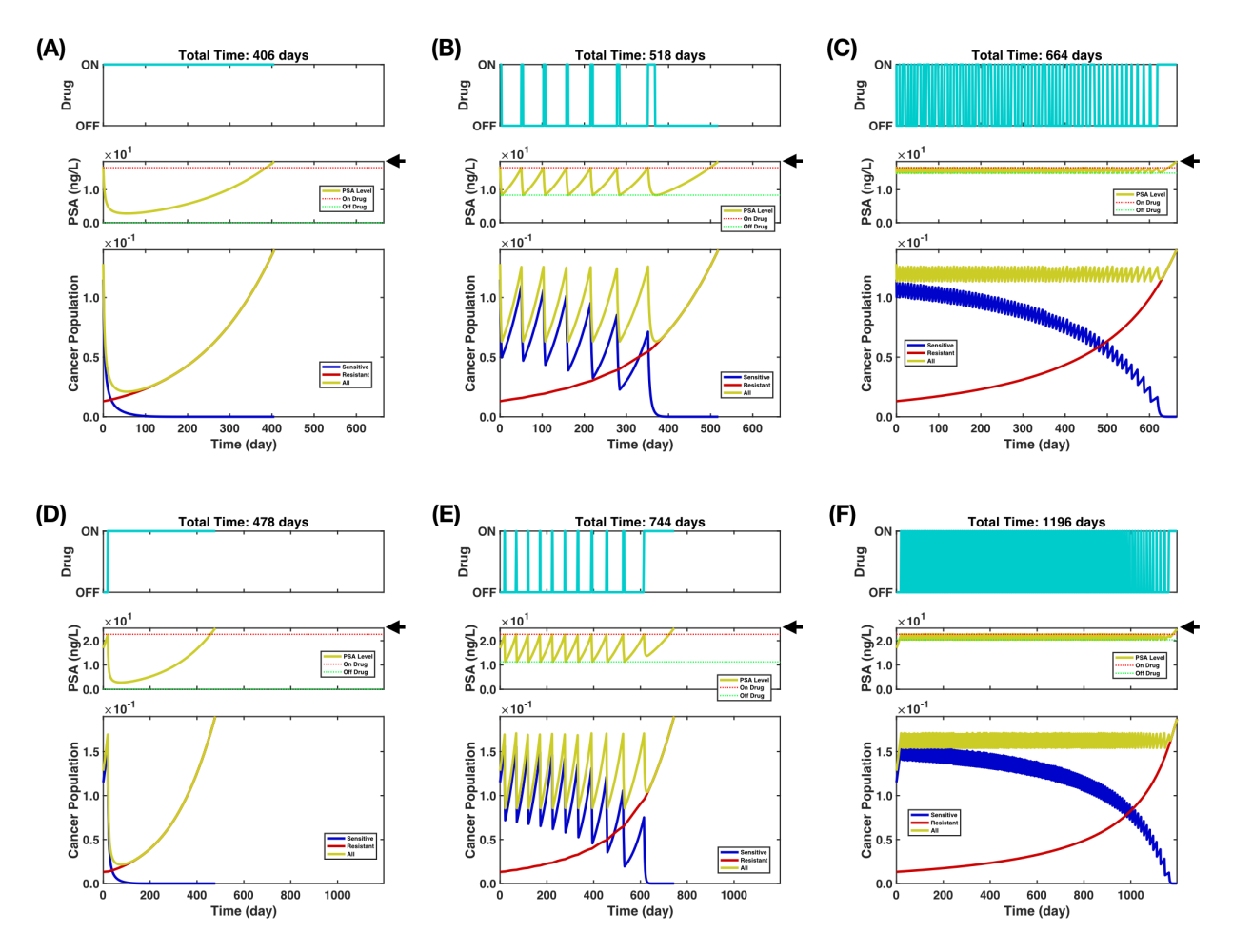


FIG. 6: Slowing down cancer progression. We explore the dynamics of cancer progression under different treatments, for small PSA thresholds i.e.  $PSA_{thr}/PSA_K = 0.14$  in  $(\mathbf{A}, \mathbf{B}, \mathbf{C})$  and 0.19 in  $(\mathbf{D}, \mathbf{E}, \mathbf{F})$ . We show the response of patient P1007 under a continuous therapy with  $\eta_{\uparrow} = 0.90$  in  $(\mathbf{A}, \mathbf{D})$ , under a continuous therapy with  $(\eta_{\uparrow}, \eta_{\downarrow}) = (0.90, 0.50)$  in  $(\mathbf{B}, \mathbf{E})$ , and under a continuous therapy with  $(\eta_{\uparrow}, \eta_{\downarrow}) = (0.90, 0.90)$  in  $(\mathbf{C}, \mathbf{F})$ . The black arrow indicates the PSA threshold level for each plot.

Appendix C, most of those are also (0.90, 0.90). We will provide an analytical justification for this finding in Section B.

B. 
$$PSA_{thr}/PSA_{K\mu} > 1/\alpha_{RS}$$

Out of N=32 patients, 27 of them have  $PSA(t_{m_{\mu}^{treat}})/PSA_{K\mu} > 1/\alpha_{RS}$ , where  $PSA(t_{m_{\mu}^{treat}})$  is the PSA levels of patient  $\mu$  when Abiraterone is first administrated (see Fig. 4C). Since  $PSA(t_{m_{\mu}^{treat}}) < PSA_{thr}$  (all patients show no symptom at  $t=t_{m_{\mu}^{treat}}$ ), this that the condition  $PSA_{thr}/PSA_{K\mu} > 1/\alpha_{RS}$  is commonly satisfied.

While the total achievable time  $\tau_{\rm tot}(\eta_{\uparrow}, \eta_{\downarrow})$  is always finite for  ${\rm PSA}_{\rm thr} < {\rm PSA}_{K\mu}/\alpha_{RS}$ , as

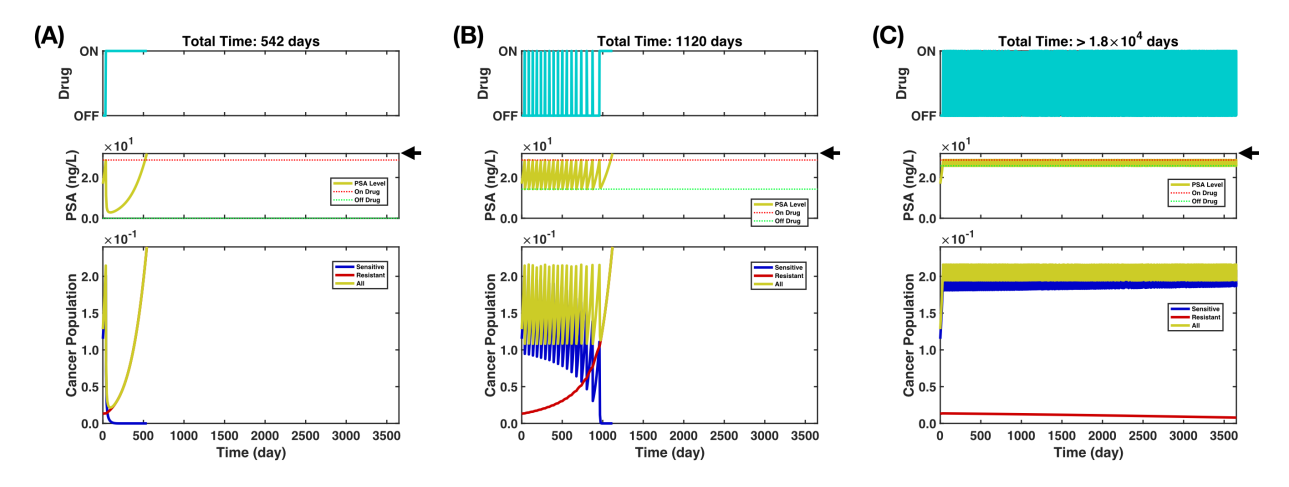


FIG. 7: Chronic cancer progression. We explore the long-time dynamics of cancer progression under different treatments, for a large PSA threshold i.e.  $PSA_{thr}/PSA_K = 0.24$ . We show the response of patient P1007 under a continuous therapy with  $\eta_{\uparrow} = 0.90$  in (A), under an adaptive therapy with  $(\eta_{\uparrow}, \eta_{\downarrow}) = (0.90, 0.50)$  in (B), and under adaptive therapy with  $(\eta_{\uparrow}, \eta_{\downarrow}) = (0.90, 0.90)$  in (C). The black arrow indicates the PSA threshold for each plot.

resistant cells will eventually dominate the cancer population after many drug administration cycles, for PSA<sub>thr</sub> > PSA<sub>Kµ</sub>/ $\alpha_{RS}$  it might become possible to keep the number of resistant cells under control forever. This can be realized only when the number of sensitive cells can reduce faster than the resistant cells can increast during the on-drug period (i.e.  $dx_S/dt + dx_R/dt < 0$ ), as we will derive in Appendix B. In other words, cancer can then shift from being a lethal disease to a chronic condition. In Fig. 7, we explore the consequences of PSA<sub>thr</sub>/PSA<sub>K</sub> = 0.24 for the same patient as in Section V A 2, on cancer progression under adaptive chemotherapy over a long time period. We find that a HLTC treatment can extend the total achievable time indefinitely (we have checked up to 50 years  $\approx 1.8 \times 10^4$  days), as illustrated in Fig. 7C. However, if the PSA off-level PSA<sub>↓</sub> is too low, a threshold breach can still occur, as seen in Fig. 7B. Continuous treatment appears to always result in negative outcomes, as shown in Fig. 7A.

What we have observed in this Section and in Section VA2 is that HLTC treatment typically leads to improved outcomes, either by maximizing the total drug response time for low PSA<sub>thr</sub> or by transforming the disease into a chronic condition for sufficiently high PSA<sub>thr</sub>. This simple insight could serve as a valuable guide for enhancing current adaptive chemotherapy treatments. We suggest that clinicians might explore the possibility of implementing HLTC, i.e. waiting for the disease to advance further rather than initiating treatment too early. It is worth mentioning that this kind of "watchful waiting" approach

before treatment is not uncommon in practice [37], at least historically. Furthermore, even without employing the "watchful waiting" approach (i.e., disregarding the *high level* component of HLTC), maintaining the current method for determining the appropriate PSA level for the initial drug treatment (that is,  $PSA_{\uparrow}$ ) but implementing a *tighter control*, may also change prostate cancer into a chronic disease for many patients (our simulation indicates that, with this approach, 19 out of 32 patients could potentially become chronic).

#### VI. DISCUSSION

Cancer has posed an immense challenge to modern medicine due to its complex nature and the absence of a definitive cure [38], casting a shadow of devastation upon those affected. This disease can wreak havoc on the human body, resulting in a multitude of severe impacts before leading to the eventual demise. While prostate cancer treatments can prolong life-expectancy, they can also be extremely aggressive and cause debilitating side effects [39]. Chemotherapy, a common treatment, frequently induces hair loss, nausea, and extreme fatigue, significantly impacting not only the physical but also the emotional well-being of patients [40]. It is crucial to understand that augmented drug administration does not always result in an increased lifespan, even at the cost of more suffering. Paradoxically, it appears plausible to significantly extend the patient life while concurrently reducing the treatment ratio (the proportion of time a drug is given compared to the total treatment duration) throughout the treatment course via adaptive chemotherapy [15]. In other words, a longer and better life may be achievable.

In this work, we use a systematic statistical method, LBEB approach for NLME, to estimate patient-informed parameters for a Stackelberg game-theoretic multi-population model that quantitatively describes prostate cancer progression [17]. We obtain estimates for common parameters across all patients as well as the probability distribution for patient-specific parameters in Section IV. We then employ a Bayesian Optimization approach to identify the optimal adaptive chemotherapeutic treatment policy for a single drug (Abiraterone) aimed at maximizing the time before the patient begins to show symptoms, under the assumption that we know how advanced the cancer needs to be for symptoms to become manifest, in Section V. We show that a high level tight control (HLTC) treatment, in which the trigger signals (i.e., the biomarker levels) for drug administration and cessation are both high and

close together, typically yields the best outcomes, as demonstrated through both computer-assisted and theoretical means (see Appendix B). Furthermore, we demonstrate that it may be possible to transform prostate cancer from a terminal disease into a chronic condition for most patients in Section V B.

Following this work, there are many directions for further exploration. First and foremost is realizing the potential benefits of HLTC adaptive therapeutic treatments in laboratory studies and clinical practice. Work along this direction is already in progress. On the numerical investigation front, we have only optimize (via Bayesian Optimization) a very simple treatment policy, in which there are only two states to be adjusted in drug administration: either no drug or the maximum dosage rate. Allowing for more structured, possibly continuous in time – not just on/off – as proposed in [41], will provide a much richer protocol space to optimize in, and hopefully, better solution to discover. Additional factors can also be considered, such as the extreme toxicity of Docetaxel [15]. Too frequent dosages can be intolerable to the patient's body. Thus, for the treatment policy, limits should be imposed on the administration of Docetaxel within a specific timeframe to ensure patient safety, which is indeed often the case in clinical practices.

Better analysis on more realistic models of cancer could also lead to new insights and novel discoveries regarding collective behavior emergence from population dynamics under ever-changing conditions [42]. Stochastic therapies (in the spirit of the Kapitza stochastic stabilization of the inverted pendulum [43, 44]) might prove more effective in targeting cancerous cells compared to periodic ones (a phenomenon observed in a robotic model system [45]). Importantly, we know that spatial dynamics are crucial in evolutionary systems [46]. Considering the metastatic nature of cancer cells, capturing how cells migrate (and also the topology of the environment the cells live in [47, 48]) in the mathematical models should be of critical importance as we strive for modeling fidelity.

#### Appendix A: Best Fit Parameters

Here, we present the best-fit parameters estimated using our LBEB approach (see Fig. 8). The patient ID numbers, labeled from 1 to 32, correspond to the following codenames (in the same order):

• Patients treated with adaptive chemotherapy: P1001, P1002, P1003, P1004, P1005,

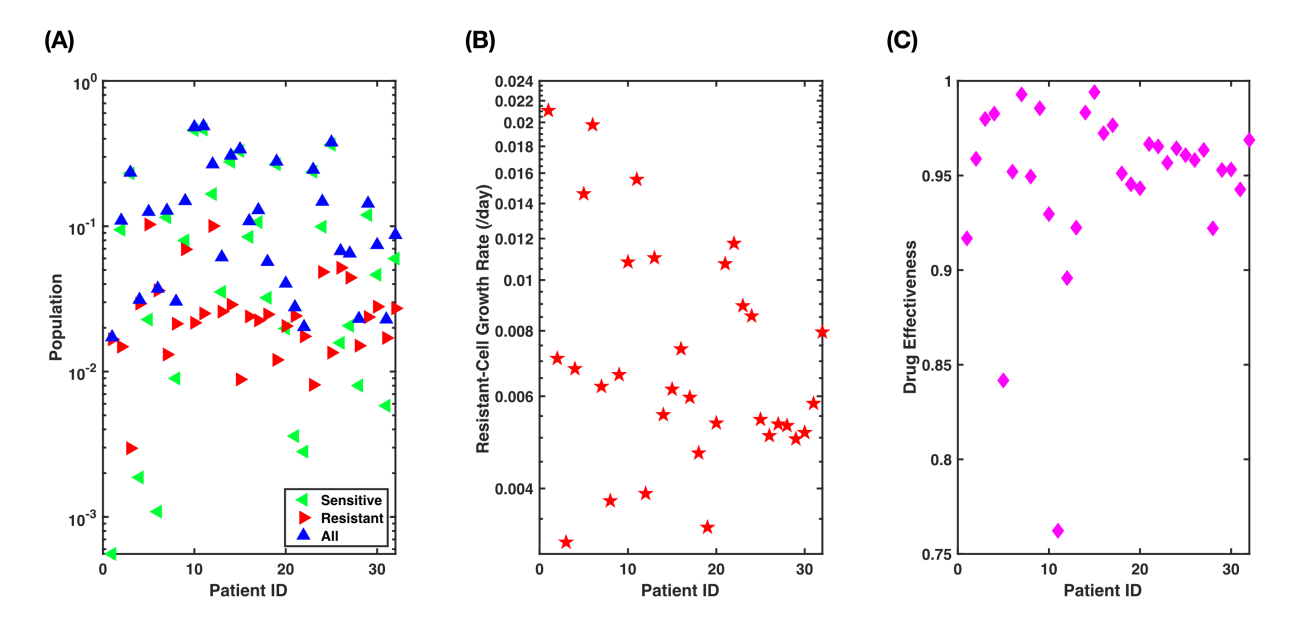


**FIG. 8:** Patient-specific parameters. Here we show the identified initial population values  $\{x_S(0), x_R(0)\}$ , the resistant cell growth rate  $r_R$ , and the drug effectiveness  $\gamma$ . (A) The initial values  $\{x_S(0), x_R(0)\}$ . The green pointing-left triangles are  $x_S(0)$ , the red pointing-right triangles are  $x_R(0)$ , and the blue pointing-up triangles are the sum  $x(0) \equiv x_S(0) + x_R(0)$ . (B) The resistant cell growth rate  $r_R$ . (C) The drug effectiveness  $\gamma$ .

P1006, P1007, P1009, P1010, P1011, P1012, P1014, P1015, P1016, P1017, P1018, P1020.

Patients treated with continuous chemotherapy: C001, C002, C003, C004, C005, C006,
 C007, C008, C009, C010, C011, C012, C013, C014, C015.

### Appendix B: An Analytical Justification for the High Level Tight Control Paradigm

The clinician aims to manage cancer progression such that the observable PSA(t) remains below a threshold PSA<sub>thr</sub> for as long as possible. This threshold corresponds to keeping the total cancer cell population below  $x_{\text{thr}} \equiv \text{PSA}_{\text{thr}}/\text{PSA}_K$ . The total achievable time  $\tau_{tot}$  until this threshold is breached is the sum of three contributions (see Fig. 9):

$$\tau_{\rm tot} = \tau_{\rm start} + \Delta \tau + \tau_{\rm cont} ,$$
 (B1)

in which we have:

•  $\tau_{\text{start}}$ : The time from when the patient begins care with the clinician (at t=0) until

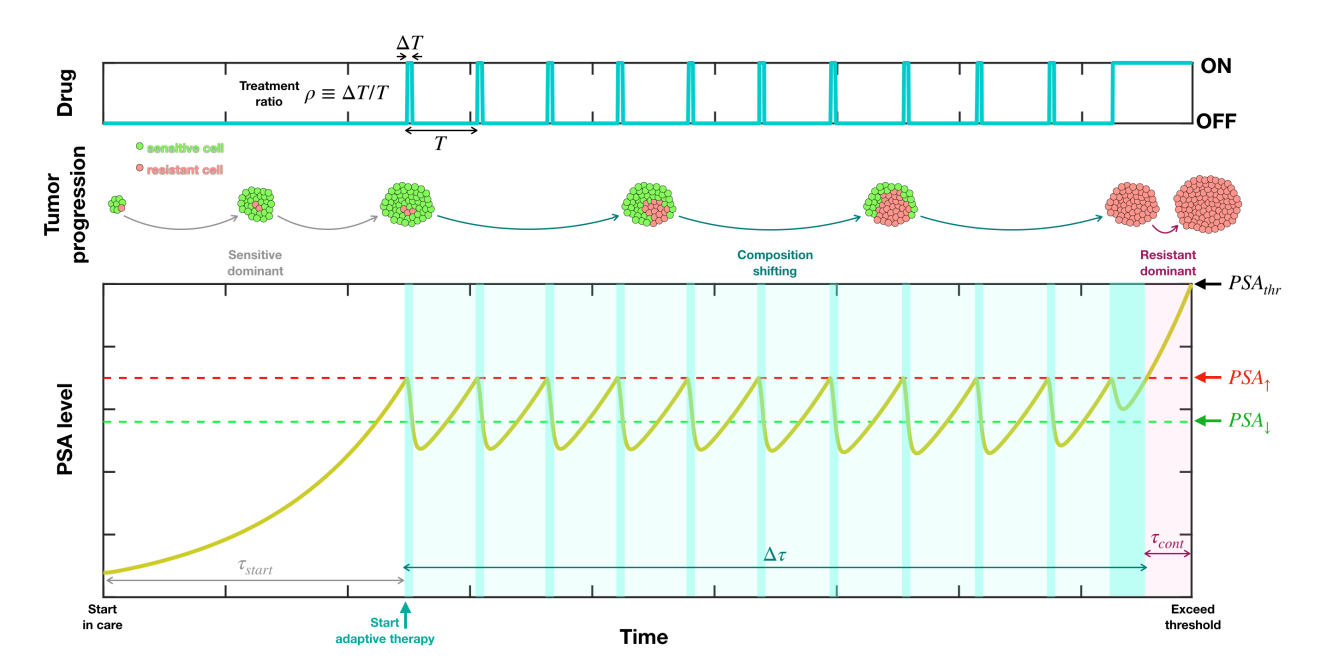


FIG. 9: Cancer progression and the changes in PSA levels observed during adaptive chemotherapy treatment. The upper plot displays drug administration. The middle plot illustrates cancer progression within a tumor, with green circles representing sensitive cells and red circles indicating resistant cells. The bottom plot tracks PSA level changes over time throughout the treatment, highlighting three distinct phases until the threshold is surpassed.

the adaptive chemotherapy starts. During this period, the growth of sensitive cells is predominantly observed.

- $\Delta\tau$ : The drug response time, from when the treatment starts to when it cannot suppress the growth of cancer cells. During this time, the composition of the cancer population shifts from being predominantly sensitive cells to being dominated by resistant cells.
- τ<sub>cont</sub>: The time from when the treatment fails to when the PSA threshold is breached.
   During this period, the patient is usually maintained on continuous Abiraterone treatment to prevent any potential regrowth of sensitive cells. Consequently, the growth of resistant cells is predominantly observed.

For a drug treatment cycle, we define the treatment ratio  $\rho$  as the fraction of the time period during that cycle in which the drug Abiraterone is administered to the patient. In other words, if the total time period of the treatment cycle is T and the *on-drug* time period is  $\Delta T$ , then  $\rho \equiv \Delta T/T$  (see Fig. 9).

#### 1. Assumptions and Approximations

To quantitatively understand why HLTC can typically maximize the total achievable time (and also reduce the average Abiraterone intake rate), let us investigate adaptive chemotherapy for prostate cancer in a simple regime to obtain some concrete analytical estimation. We assume that  $\alpha_{RS}x_S(t)$  is much larger compared to  $x_R(t)$  before Abiraterone first administrated i.e.  $t \in [0, \tau_{\text{start}}]$ . This condition holds true for most patients at t = 0 (as shown in Fig. 4B) and therefore at later time, since the ratio  $x_S(t)/x_R(t)$  is always increase with time. We can derive that from Eq. (4), as the growth of sensitive cells is always faster:

$$r_S \{1 - [x_S(t) + x_R(t)]\} > r_R \{1 - [x_R(t) + \alpha_{RS}x_S(t)]\},$$
 (B2)

in which the ecological competition coefficient  $\alpha_{RS} \approx 5.2 \gg 1$  and the growth rate ratio  $\beta \equiv r_S/r_R \approx 3.0$  (as estimated in Section IV C). We also assume that PSA<sub>thr</sub> is much smaller than PSA<sub>K</sub>, which remains reasonable even when even when PSA<sub>thr</sub>  $\lesssim$  PSA<sub>K</sub>/ $\alpha_{RS}$ . Denote the cancer cell population when the biomarker reaches the *on-level* to be  $x_{\uparrow} \equiv \text{PSA}_{\uparrow}/\text{PSA}_K$ , then  $x_{\uparrow} \leq x_{\text{thr}}$ . We therefore have  $x_S(t), x_R(t), x_{\uparrow} \ll 1$  during  $t \in [0, \tau_{\text{tot}}]$ ; however, it is important to note that  $\alpha_{RS}x_S(t)$  does not necessarily have to be negligible. These above assumptions allow us to approximate Eq. (4) for  $t \in [0, \tau_{\text{start}}]$  as:

$$\frac{d}{dt}x_S(t) \approx r_S x_S(t) ,$$

$$\frac{d}{dt}x_R(t) \approx r_R \left[1 - \alpha_{RS} x_S(t)\right] x_R(t) .$$
(B3)

These ODEs can be solved analytically for  $x_S(t)$  and  $x_R(t)$ , given the initial values  $x_S(0)$  and  $x_R(0)$ :

$$x_S(t) = x_S(0) \exp(r_S t)$$
,  $x_R(t) = x_R(0) \exp(r_R t) \exp\left\{-\frac{\alpha_{RS}}{\beta} \left[x_S(t) - x_S(0)\right]\right\}$ . (B4)

To obtain  $\tau_{\text{start}}$ , we have to solve:

$$x_S(\tau_{\text{start}}) + x_R(\tau_{\text{start}}) = x_{\uparrow} ,$$
 (B5)

which is not analytically solvable in a general case. Let us further assume that the number of sensitive cancer cells dominates when the drug treatment begins i.e.  $x_S(\tau_{\text{start}}) \gg x_R(\tau_{\text{start}})$ , so that  $x_S(\tau_{\text{start}}) \approx x_{\uparrow}$ . We can then obtain a simple approximation for  $\tau_{\text{start}}$ :

$$\tau_{\text{start}} \approx \ln \left[ \frac{x_{\uparrow}}{x_S(0)} \right] r_S^{-1} .$$
(B6)

Plug this back to Eq. (B4), we get the resistant cell population at that time to be:

$$x_R(\tau_{\text{start}}) = x_R(0) \left[ \frac{x_{\uparrow}}{x_S(0)} \right]^{1/\beta} \exp\left\{ -\frac{\alpha_{RS}}{\beta} \left[ x_{\uparrow} - x_S(0) \right] \right\} . \tag{B7}$$

If the initial total cancer cell population is small  $x(0) \ll x_{\uparrow}$ , then even with  $x_S(0) \sim x_R(0)$ , the condition  $x_S(\tau_{\text{start}}) \sim x_{\uparrow} \gg x_R(\tau_{\text{start}})$  will still hold. Another way for this condition to arise is if the sensitive cell population initially dominates, meaning  $x_S(0) \gg x_R(0)$ .

We study an adaptive therapy operates between the biomarker levels  $PSA_{\uparrow}$  and  $PSA_{\downarrow} = (1 - \epsilon)PSA_{\uparrow}$ . This means the total cancer cell population x(t) is is maintained between  $x_{\uparrow}$  and  $x_{\uparrow}(1 - \epsilon)$ . Note that from Eq. (8), we can relate this control window parameter with the off-drug policy parameter via  $\epsilon = 1 - \eta_{\downarrow}$ . For a tight control  $\epsilon \ll 1$ , we can assume that during the adaptive treatment time period  $t \in [\tau_{\text{start}}, \tau_{\text{exit}}]$  (where  $\tau_{\text{exit}} \equiv \tau_{\text{start}} + \Delta t$ ), the cancer population is, on average, stabilized at:

$$x(t) \approx x_{\uparrow} \left( 1 - \frac{\epsilon}{2} \right) \implies x_S(t) \approx x_{\uparrow} \left( 1 - \frac{\epsilon}{2} \right) - x_R(t) .$$
 (B8)

This assumption only holds when  $\langle dx/dt \rangle = 0$  is possible, where  $\langle \circ \rangle$  denotes the average of a quantity  $\circ$  over time during a drug treatment cycle. Since the number of cells always increase during the *off-drug* time period, we need to have during the *on-drug* the following inequality:

$$\frac{d}{dt}x_S(t)\Big|_{\Lambda(t)=1} + \frac{d}{dt}x_R(t) \le 0.$$
(B9)

We use Eq. (4) to rewrite this as:

$$r_{S}\left\{1 - \left[\frac{x_{S}(t) + x_{R}(t)}{1 - \gamma}\right]\right\} x_{S}(t) + r_{R}\left\{1 - \left[x_{R}(t) + \alpha_{RS}x_{S}(t)\right]\right\} x_{R}(t) \le 0$$

$$\implies \left\{\left[\frac{1 - x_{\uparrow}\left(1 - \frac{\epsilon}{2}\right)}{x_{S}(t)}\right] - (\alpha_{RS} - 1)\right\} x_{R}(t) \le \beta \left\{\left[\frac{x_{\uparrow}\left(1 - \frac{\epsilon}{2}\right)}{1 - \gamma}\right] - 1\right\}.$$
(B10)

For most patients,  $\gamma \to 1$  (see Fig. 4A and Fig. 8C). Together with Eq. (B8) and the assumption  $x_S(t), x_R(t), x_{\uparrow} \ll 1$  previously mentioned, this inequality becomes:

$$x_S(t) \ge \frac{x_{\uparrow}}{\beta} \left\{ \left[ \frac{x_{\uparrow} \left( 1 - \frac{\epsilon}{2} \right)}{1 - \gamma} \right] - 1 \right\}^{-1} \approx \frac{1 - \gamma}{\beta \left( 1 - \frac{\epsilon}{2} \right)} . \tag{B11}$$

The right hand side is a finite positive value very close to 0, which is also increasing with  $\epsilon$ . This means that the tighter the control (i.e. the smaller the control window), the more difficult it becomes to maintain stabilization Eq. (B8), as it reduces the allowable range

for  $x_S$ . Therefore, when the adaptive treatment starts failing to suppress the cancer growth (i.e. the inequality does not hold anymore), we can make the following approximation:

$$x_S(\tau_{\text{exit}}) \approx 0 \implies x_R(\tau_{\text{exit}}) \approx x_{\uparrow} \left(1 - \frac{\epsilon}{2}\right) ,$$
 (B12)

which is consistent with the behavior seen in Fig. 6B,C,E,F and Fig. 7B. In summary, during the adaptive treatment time period  $t \in [\tau_{\text{start}}, \tau_{\text{exit}}]$ , the growth of Abiraterone resistant cells obeys:

$$\frac{d}{dt}x_R(t) = r_R \left\{ \left[ 1 - \alpha_{RS}x_{\uparrow} \left( 1 - \frac{\epsilon}{2} \right) \right] - (1 - \alpha_{RS})x_R(t) \right\} x_R(t) , \qquad (B13)$$

which comes from Eq. (4) and the stabilization Eq. (B8), until  $x_R(t)$  reaches  $x_{\uparrow}$ . The solution of this ODE is given by:

$$r_R \left[ 1 - \alpha_{RS} x_{\uparrow} \left( 1 - \frac{\epsilon}{2} \right) \right] (t - \tau_{\text{start}}) = \ln \left\{ \frac{x_R}{1 - \left[ \frac{1 - \alpha_{RS}}{1 - \alpha_{RS} x_{\uparrow} \left( 1 - \frac{\epsilon}{2} \right)} \right] x_R} \right\} \Big|_{x_R(\tau_{\text{start}})}^{x_R(t)} . \tag{B14}$$

To obtain  $\Delta \tau$  we need to solve:

$$\Delta \tau = \ln \left\{ \frac{x_R}{1 - \left[ \frac{1 - \alpha_{RS}}{1 - \alpha_{RS} x_{\uparrow} \left( 1 - \frac{\epsilon}{2} \right)} \right] x_R} \right\} \begin{vmatrix} x_{\uparrow} \left( 1 - \frac{\epsilon}{2} \right) \\ x_{R} \left( \tau_{\text{start}} \right) \end{vmatrix} \left[ \frac{r_R^{-1}}{1 - \alpha_{RS} x_{\uparrow} \left( 1 - \frac{\epsilon}{2} \right)} \right] , \quad (B15)$$

in which for  $x_R(\tau_{\rm start}) \ll x_{\uparrow} \ll 1$  can help us to further approximate this expression to:

$$\Delta \tau \approx \ln \left\{ \frac{x_{\uparrow} \left( 1 - \frac{\epsilon}{2} \right) \left[ 1 - \alpha_{RS} x_{\uparrow} \left( 1 - \frac{\epsilon}{2} \right) \right]}{x_{R} (\tau_{\text{start}})} \right\} \left[ \frac{r_{R}^{-1}}{1 - \alpha_{RS} x_{\uparrow} \left( 1 - \frac{\epsilon}{2} \right)} \right] . \tag{B16}$$

For the last phase  $t \in [\tau_{\text{exit}}, \tau_{\text{tot}}]$ , the resistant cancer cells has taken over the population, the cancer progression can be described with  $x(t) = x_R(t)$  and the ODE:

$$\frac{d}{dt}x_R(t) \approx r_R \left[1 - x_R(t)\right] x_R(t) , \qquad (B17)$$

which can be obtained from the Eq. (4) after setting  $x_S(t) = 0$ . This ODE can be solved analytically to give:

$$r_R(t - \tau_{\text{exit}}) = \ln \left[ \frac{x_R}{1 - x_R} \right] \Big|_{x_R(\tau_{\text{exit}})}^{x_R(t)} . \tag{B18}$$

To obtain  $\tau_{\rm cont}$  we need to solve:

$$\tau_{\text{cont}} = \ln \left[ \frac{x_R}{1 - x_R} \right] \Big|_{x_{\uparrow} \left(1 - \frac{\epsilon}{2}\right)}^{x_{\text{thr}}} r_R^{-1} , \qquad (B19)$$

in which we can use  $x_{\rm thr} \ll 1$  to to approximate its value to be:

$$\tau_{\rm cont} = \ln \left[ \frac{x_{\rm thr}}{x_{\uparrow} \left( 1 - \frac{\epsilon}{2} \right)} \right] r_R^{-1} .$$
(B20)

# 2. An Analytical Expression for the Treatment Ratio $\rho$ and the Total Achievable Time $\tau_{\rm tot}$

a. The Treatment Ratio  $\rho$ 

Define the following averaging during a drug treatment cycle:

$$\Omega \equiv \left\langle \frac{1}{1 - \gamma \Lambda(t)} \right\rangle = \rho \times \left( \frac{1}{1 - \gamma} \right) + (1 - \rho) \times 1$$

$$= 1 + \left( \frac{\gamma}{1 - \gamma} \right) \rho \implies \rho = \left( \frac{1 - \gamma}{\gamma} \right) (\Omega - 1) , \tag{B21}$$

so that when Eq. (B8) holds, we can use Eq. (4) to obtain:

$$\frac{d}{dt} [x_S + x_R] = r_S \left[ 1 - \Omega \left( x_S + x_R \right) \right] x_S + r_R \left[ 1 - \left( x_R + \alpha_{RS} x_S \right) \right] x_R = 0$$

$$\implies \rho = \left( \frac{1 - \gamma}{\gamma} \right) \left( \left\{ \frac{1 - \frac{x_R}{\beta x_S} \left[ 1 - \left( x_R + \alpha_{RS} x_S \right) \right]}{x_{\uparrow} \left( 1 - \frac{\epsilon}{2} \right)} \right\} - 1 \right) . \tag{B22}$$

If the resistant cell population is negligible i.e.  $x_R \ll x_S$  (and note that  $\gamma \to 1$  for most patients) then this expression can be further simplified:

$$\rho \approx \frac{1 - \gamma}{x_{\uparrow} \left( 1 - \frac{\epsilon}{2} \right)} \ . \tag{B23}$$

This implies the tightest control window  $\epsilon$  (thus the maximum policy parameter  $\eta_{\downarrow}$ ) will give the smallest treatment ratio  $\rho$ .

#### b. The Total Achievable Time $\tau_{tot}$

The total achievable time can be calculated from the sum of the times given in Eq. (B6), Eq. (B16), and Eq. (B20); however, the resulting expression is quite complex. In the limit of very small resistant cells in the beginning  $x_R(0) \to 0$ , the formula for  $\tau_{\text{tot}}$  is simple and can be splitted into two parts:

$$\tau_{\text{tot}} = \tau_{\text{tot}}^{(c)} + \tau_{\text{tot}}^{(a)} . \tag{B24}$$

The part  $\tau_{\text{tot}}^{(c)}$  is equal to the *total achievable time* if a continuous drug treatment is applied from the beginning, while  $\tau_{\text{tot}}^{(a)}$  represents the additional time gained by using an adaptive chemotherapeutic treatment (for a given control window  $\epsilon$  and *on*-drug level PSA<sub>\(\text{\tot}\)</sub>) instead:

$$\tau_{\text{tot}}^{(c)} \approx \ln \left[ \frac{x_{\text{thr}}}{(1 - x_{\text{thr}}) x_R(0)} \right] r_R^{-1} ,$$

$$\tau_{\text{tot}}^{(a)} \approx \left[ \frac{\alpha_{RS} x_{\uparrow} \left( 1 - \frac{\epsilon}{2} \right)}{1 - \alpha_{RS} x_{\uparrow} \left( 1 - \frac{\epsilon}{2} \right)} \right] \ln \left\{ \frac{x_{\uparrow}}{\left[ 1 - x_{\uparrow} \left( 1 - \frac{\epsilon}{2} \right) \right] x_R(0)} \right\} r_R^{-1} .$$
(B25)

Consider increasing the  $x_{\text{thr}}$  but does not let it surpasses  $1/\alpha_{RS}$ , then maximum time gained corresponds to the *tightest control* (i.e. smallest possible  $\epsilon$ ) and the *highest* PSA on-drug level below the threshold (i.e. largest allowable  $x_{\uparrow}$ ):

$$\max \tau_{\text{tot}}^{(a)} \le \tau_{\text{tot}}^{(a)}(0, x_{\text{thr}}) = \left(\frac{\alpha_{RS} x_{\text{thr}}}{1 - \alpha_{RS} x_{\text{thr}}}\right) \tau_{\text{tot}}^{(c)}. \tag{B26}$$

This description is that of the HLTC treatment. If we let  $x_{\text{thr}}$  exceed  $1/\alpha_{RS}$ , then max  $\tau_{\text{tot}}^{(a)}$  can be infinitely large, indicating that the cancer disease can become chronic. Note that for this to occur, the total number of cancer cells must be stabilized, as indicated in Eq. (B8). This stabilization can fail if the population of sensitive cells is too low, as explained in Eq. (B11).

We have made several assumptions and approximations to reach the conclusions outlined above. While our findings may not be universally applicable, they can serve as a valuable guide, as they agrees with the optimal treatment strategy for most cases (41 out of 43) discussed in Appendix C.

#### Appendix C: Optimal Treatment Policy Report

We report the optimal adaptive therapy treatment policy parameters  $(\eta_{\uparrow}^*, \eta_{\downarrow}^*)$  found by employing a Bayesian optimization approach, with different values of the PSA threshold i.e.  $PSA_{thr}/PSA_K = 0.14$  in Table I and  $PSA_{thr}/PSA_K = 0.19$  in Table II. After the results found in Section V A 2, instead of select  $n_{\text{eval}} = 10$  random points to evaluate at the beginning, we do that for  $n_{\text{eval}} - 2 = 8$  and let the last two points to be  $(\eta_{\uparrow}, \eta_{\downarrow}) = (0.00, 0.00)$  (representing a continuous treatment start at t = 0) and  $(\eta_{\uparrow}, \eta_{\downarrow}) = (0.90, 0.90)$  (representing a HLTC treatment).

There is only one patient that has  $(\eta_{\uparrow}^*, \eta_{\downarrow}^*) \neq (0.90, 0.90)$  for both of these  $PSA_{thr}/PSA_K$ , which is patient P1005. Upon closer examination, we find that this patient has very low drug

Patient ID	$\eta_{\uparrow}^*$	$\eta_{\downarrow}^{*}$	$ au_{\mathrm{tot}}(\eta_{\uparrow}^*, \eta_{\uparrow}^*)$	$\tau_{\rm tot}(0.90, 0.90)$	$\tau_{\rm tot}(0.00, 0.00)$
P1001	0.90	9.00	112	112	108
P1002	0.90	0.90	544	544	376
P1004	0.90	0.90	271	271	249
P1005	0.22	0.81	10	10	10
P1006	0.90	0.90	76	76	74
P1007	0.90	0.90	664	664	406
P1009	0.90	0.90	680	680	555
P1015	0.90	0.90	223	223	189
P1018	0.90	0.90	382	382	271
P1020	0.90	0.90	495	495	345
C001	0.90	0.90	556	556	431
C003	0.90	0.90	531	531	418
C004	0.90	0.90	205	205	177
C005	0.90	0.90	228	228	191
C009	0.90	0.90	248	248	223
C010	0.90	0.90	285	285	244
C011	0.90	0.90	593	593	495
C013	0.90	0.90	474	474	370
C014	0.90	0.90	494	494	405
C015	0.90	0.90	317	317	234

TABLE I:  $PSA_{thr}/PSA_K = 0.14$ 

effectiveness, indicating that for the PSA threshold values we investigated, it is preferable to initiate treatment as soon as possible. In Fig. 10, we show the PSA progressions under  $PSA_{thr}/PSA_K = 0.19$ , for the adaptive treatment using HLTC  $(\eta_{\uparrow}, \eta_{\downarrow}) = (0.90, 0.90)$  and for the optimal treatment  $(\eta_{\uparrow}^*, \eta_{\downarrow}^*)$  identified by our Bayesian optimization approach. Note that  $PSA_{\uparrow}$  for the found optimal treatment is already below PSA(0), and PSA(t) does not decrease, indicating that it is effectively equivalent to a continuous treatment initiated from the very beginning at t = 0.

Patient ID	$\eta_{\uparrow}^*$	$\eta_{\downarrow}^*$	$\tau_{\text{tot}}(n_{\star}^*, n_{\star}^*)$	$\tau_{\rm tot}(0.90, 0.90)$	$\tau_{\text{tot}}(0.00, 0.00)$
P1001	'	0.90	$\frac{147}{147}$	147	126
P1002		0.90	959	959	427
P1004		0.90	358	358	303
P1005		0.68	45	38	45
P1006		0.90	101	101	93
P1007		0.90	1196	1196	464
P1009		0.90	1005	1005	652
P1010		0.90	244	244	177
P1015		0.90	365	365	230
P1018	0.90	0.90	646	646	320
P1020	0.90	0.90	853	853	406
C001	0.90	0.90	884	884	511
C003	0.90	0.90	831	831	489
C004	0.90	0.90	282	282	211
C005	0.90	0.90	316	316	221
C007	0.90	0.90	295	295	191
C009	0.90	0.90	377	377	296
C010	0.90	0.90	435	435	313
C011	0.90	0.90	913	913	579
C012	0.90	0.90	985	985	511
C013	0.90	0.90	769	769	442
C014	0.90	0.90	724	724	470
C015	0.90	0.90	522	522	280

TABLE II:  $PSA_{thr}/PSA_K = 0.19$ 

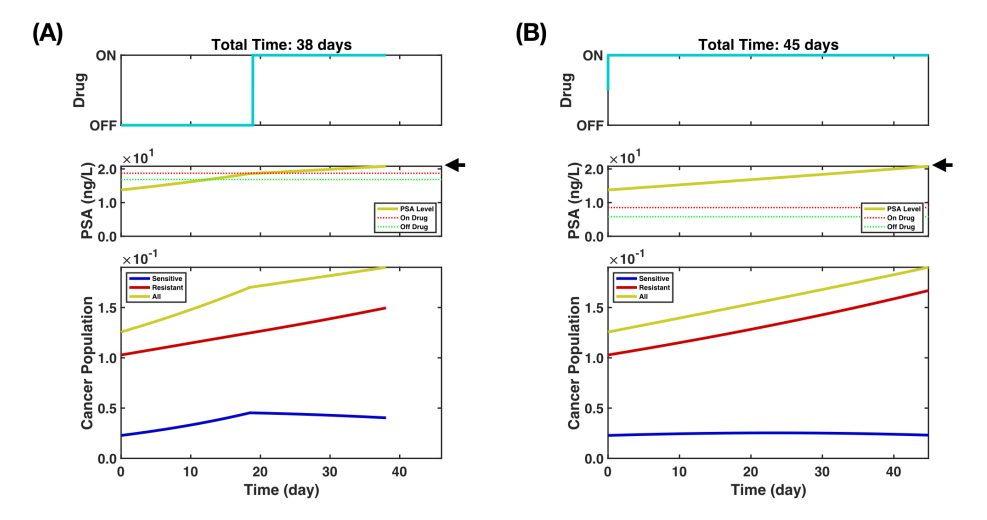


FIG. 10: Cancer progression of patient P1005 under the PSA threshold  $PSA_{thr}/PSA_K = 0.19$ . This patient has a low drug effectiveness parameters, so that when the drug is administrated early, it only has a small impact. We show the response of this patient P1007 under the HLTC adaptive therapy with  $(\eta_{\uparrow}, \eta_{\downarrow}) = (0.90, 0.90)$  in (A) (A), and under the optimal adaptive therapy (identified via Bayesian optimization) with  $(\eta_{\uparrow}^*, \eta_{\downarrow}^*) = (0.41, 0.68)$  in (B), which is equivalent to a continuous treatment started from the very beginning. The black arrow indicates the PSA threshold for each plot.

A. B. Turke, K. Zejnullahu, Y.-L. Wu, Y. Song, D. Dias-Santagata, E. Lifshits, L. Toschi,
 A. Rogers, T. Mok, L. Sequist, et al., Cancer cell 17, 77 (2010).

- [3] A. Sottoriva, H. Kang, Z. Ma, T. A. Graham, M. P. Salomon, J. Zhao, P. Marjoram, K. Siegmund, M. F. Press, D. Shibata, et al., Nature genetics 47, 209 (2015).
- [4] D. M. Fitzgerald, P. Hastings, and S. M. Rosenberg, Annual Review of Cancer Biology 1, 119 (2017).
- [5] A. A. Hoffmann and M. J. Hercus, Bioscience **50**, 217 (2000).
- [6] A. N. Hata, M. J. Niederst, H. L. Archibald, M. Gomez-Caraballo, F. M. Siddiqui, H. E. Mulvey, Y. E. Maruvka, F. Ji, H.-e. C. Bhang, V. Krishnamurthy Radhakrishna, et al., Nature medicine 22, 262 (2016).
- [7] M. Ramirez, S. Rajaram, R. J. Steininger, D. Osipchuk, M. A. Roth, L. S. Morinishi, L. Evans,
   W. Ji, C.-H. Hsu, K. Thurley, et al., Nature communications 7, 10690 (2016).

<sup>[2]</sup> H.-e. C. Bhang, D. A. Ruddy, V. Krishnamurthy Radhakrishna, J. X. Caushi, R. Zhao, M. M. Hims, A. P. Singh, I. Kao, D. Rakiec, P. Shaw, et al., Nature medicine 21, 440 (2015).

- [8] J. Qin, X. Liu, B. Laffin, X. Chen, G. Choy, C. R. Jeter, T. Calhoun-Davis, H. Li, G. S. Palapattu, S. Pang, et al., Cell stem cell 10, 556 (2012).
- [9] C. J. Ercole, P. H. Lange, M. Mathisen, R. K. Chiou, P. K. Reddy, and R. L. Vessella, The Journal of urology 138, 1181 (1987).
- [10] J. R. Prensner, M. A. Rubin, J. T. Wei, and A. M. Chinnaiyan, Science translational medicine 4, 127rv3 (2012).
- [11] J. S. De Bono, C. J. Logothetis, A. Molina, K. Fizazi, S. North, L. Chu, K. N. Chi, R. J. Jones, O. B. Goodman Jr, F. Saad, et al., New England Journal of Medicine 364, 1995 (2011).
- [12] R. A. Gatenby, A. S. Silva, R. J. Gillies, and B. R. Frieden, Cancer research 69, 4894 (2009).
- [13] A. Stein, M. Salvioli, H. Garjani, J. Dubbeldam, Y. Viossat, J. S. Brown, and K. Staňková, Philosophical Transactions of the Royal Society B: Biological Sciences 378, 20210495 (2023), https://royalsocietypublishing.org/doi/pdf/10.1098/rstb.2021.0495.
- [14] J. West, L. You, J. Zhang, R. A. Gatenby, J. S. Brown, P. K. Newton, and A. R. Anderson, Cancer research 80, 1578 (2020).
- [15] J. B. West, M. N. Dinh, J. S. Brown, J. Zhang, A. R. Anderson, and R. A. Gatenby, Clinical Cancer Research 25, 4413 (2019).
- [16] E. Hansen and A. F. Read, Cancers 12, 10.3390/cancers12123556 (2020).
- [17] J. Zhang, J. Cunningham, J. Brown, and R. Gatenby, Elife 11, e76284 (2022).
- [18] J. E. Oesterling, D. C. Rice, W. J. Glenski, and E. J. Bergstralh, Urology 42, 276 (1993).
- [19] R. B. Ge, Z. W. Wang, and L. Cheng, Npj Precision Oncology 6 (2022), 0z0sc Times Cited:50 Cited References Count:138.
- [20] J. S. Zhang, J. J. Cunningham, J. S. Brown, and R. A. Gatenby, Nature Communications 8 (2017), fn9yp Times Cited:235 Cited References Count:36.
- [21] K. Fizazi, N. Tran, L. Fein, N. Matsubara, A. Rodriguez-Antolin, B. Y. Alekseev, M. Özgüroğlu, D. Ye, S. Feyerabend, A. Protheroe, et al., New England Journal of Medicine 377, 352 (2017).
- [22] K. Hashimoto, H. Tabata, T. Shindo, T. Tanaka, J. Hashimoto, R. Inoue, T. Muranaka, H. Hotta, M. Yanase, Y. Kunishima, et al., in Urologic Oncology: Seminars and Original Investigations, Vol. 37 (Elsevier, 2019) pp. 485–491.
- [23] M. J. Lindstrom and D. M. Bates, Biometrics, 673 (1990).
- [24] T. M. Inc., Matlab version: 9.14.0.2239454 (r2023a) (2023).

- [25] E. L. Crow and K. Shimizu, Lognormal distributions (Marcel Dekker New York, 1987).
- [26] D. C. Montgomery, E. A. Peck, and G. G. Vining, Introduction to linear regression analysis (John Wiley & Sons, 2021).
- [27] B. Efron, Journal of the American Statistical Association 73, 113 (1978).
- [28] R. Anderson-Sprecher, The American Statistician 48, 113 (1994).
- [29] O. Schabenberger and F. J. Pierce, Contemporary statistical models for the plant and soil sciences (CRC press, 2001).
- [30] D. McFadden, Conditional logit analysis of qualitative choice behavior (1972).
- [31] T. J. Smith and C. M. McKenna, Multiple Linear Regression Viewpoints 39, 17 (2013).
- [32] A.-N. Spiess and N. Neumeyer, BMC pharmacology 10, 1 (2010).
- [33] S. V. Archontoulis and F. E. Miguez, Agronomy Journal 107, 786 (2015).
- [34] P. I. Frazier, arXiv preprint arXiv:1807.02811 (2018).
- [35] M. A. Oliver and R. Webster, International Journal of Geographical Information System 4, 313 (1990).
- [36] E. Schulz, M. Speekenbrink, and A. Krause, Journal of Mathematical Psychology 85, 1 (2018).
- [37] A. Chapple, S. Ziebland, A. Herxheimer, A. McPherson, S. Shepperd, and R. Miller, BJU international 90, 257 (2002).
- [38] E. C. Hayden et al., Nature 455, 148 (2008).
- [39] V. Schirrmacher, International journal of oncology 54, 407 (2019).
- [40] M. S. Aslam, S. Naveed, A. Ahmed, Z. Abbas, I. Gull, and M. A. Athar, Journal of Cancer Therapy 2014 (2014).
- [41] J. J. Cunningham, J. S. Brown, R. A. Gatenby, and K. Staňková, Journal of theoretical biology 459, 67 (2018).
- [42] T. V. Phan, G. Wang, T. K. Do, I. G. Kevrekidis, S. Amend, E. Hammarlund, K. Pienta, J. Brown, L. Liu, and R. H. Austin, Journal of Biological Physics 47, 387 (2021).
- [43] P. Kapitza, Zh. Eksp. Teor. Fiz **21**, 588 (1951).
- [44] J. Sanz-Serna, Stochastics & Dynamics 8 (2008).
- [45] G. Wang, T. V. Phan, S. Li, J. Wang, Y. Peng, G. Chen, J. Qu, D. I. Goldman, S. A. Levin, K. Pienta, et al., Proceedings of the National Academy of Sciences 119, e2120019119 (2022).
- [46] A. Wu, K. Loutherback, G. Lambert, L. Estévez-Salmerón, T. D. Tlsty, R. H. Austin, and J. C. Sturm, Proceedings of the National Academy of Sciences 110, 16103 (2013).

- [47] T. V. Phan, R. Morris, M. E. Black, T. K. Do, K.-C. Lin, K. Nagy, J. C. Sturm, J. Bos, and R. H. Austin, Physical Review X 10, 031017 (2020).
- [48] T. V. Phan, S. Li, D. Ferreris, R. Morris, J. Bos, B. Gou, S. Martiniani, P. Chaikin, Y. G. Kevrekidis, and R. H. Austin, arXiv preprint arXiv:2401.16691 (2024).